LIQUID NITROGEN POWERED PRIME MOVER USING MODIFIED FOUR STROKE CYCLE ENGINE AS AN EXPANSION ENGINE

DISSERTATION SUBMITTED IN PARTIAL FULFILLMENT OF THE REQUIREMENTS FOR THE AWARD OF MASTER OF ENGINEERING

IN

THERMAL ENGINEERING

BY

S. ATHIMOOLA KRISHNAN

UNDER THE GUIDANCE OF

DR. S. MAJI
PROFESSOR IN MECHANICAL ENGINEERING
DELHI COLLEGE OF ENGINEERING
DELHI

SHRI. T. S. DATTA
HEAD, CRYOGENIC LAB
NUCLEAR SCIENCE CENTRE
NEW DELHI

DEPARTMENT OF MECHANICAL ENGINEERING
DELHI COLLEGE OF ENGINEERING
UNIVERSITY OF DELHI
DELHI

JANUARY 2005

Certificate

This is to certify that the dissertation entitled "**Liquid Nitrogen Powered Prime Mover Using Modified Four Stroke Cycle Engine as an Expansion Engine**" submitted by **S. Athimoola Krishnan** towards the partial fulfillment of the requirements for the award of **Master of Engineering in Thermal Engineering.** This is a bonfide record of his work carried out under the supervision and guidance of undersigned. It is also certified that this report has not been submitted for any other degree or diploma in any other college to the best of my knowledge.

Dr. S. Maji
Professor in Mechanical Engineering
Delhi College of Engineering
Delhi

Shri. T.S. Datta
Head, Cryogenic Lab
Nuclear Science Centre
New Delhi

Acknowledgements

The author wishes to express his deep and sincere gratitude to Prof. S. Maji for his inspiring and enthusiastic guidance throughout the course of this project work.

I am grateful to Prof. P. B. Sharma, the Principal, Delhi College of Engineering for showing his personal interest, visiting to Nuclear Science Centre, spending his valuable time to evaluate, motivate and providing guidance.

Thanks are also extended to the faculties and staff members of the Mechanical Engineering Department for extending all types of necessary support from time to time.

It is my pleasant duty to acknowledge Shri. T. S. Datta**,** Head, Cryogenic lab and Dr. A. Roy, Director, Nuclear Science Centre for granting permission to take up this project and their guidance during this project work.

I like to put my sincere thanks to Mr. Manoj Kumar, Mr. Sunder Rao, Mr. S.K. Saini, Mr. R.S. Meena and other members of the cryogenic lab and workshop for their continuous support and co-operation in making this experimental setup.

I thank my friend Dr. K. Asokan, Scientist, NSC and my brother S. Shenba Sehtupathy, A.E, HAL for their personal support during this course of study and project work.

My special thanks to Mr. Mantoo Kumar, Mr. Pradeep and Mr. Amit Verma, B.Tech (Chemical Engg.) student from Lucknow Engineering College, for their technical work and co-operation during this project.

Lastly, I thank all of my colleagues, who were involved directly and indirectly in making this project successful.

Contents

Abstract

The major concern of using conventional gasoline and diesel fuel powered I.C.engine is air pollution especially in urban areas. Even with state-of the art technology, it is not possible to eliminate toxic emission of carbon monoxides, volatile organic compounds, oxides of nitrogen and suspended particulate matter. The university of North Texas and the University of Washington independently demonstrated LN2 as a non-polluting vehicular fuel.

A heat engine that operates between atmospheric temperature as a heat source and cryogenic temperature as a heat sink is called cryogenic heat engine. A liquid nitrogen powered engine is a best alternative zero emission engine concept compared to battery operated one. The purpose of this project is to develop and demonstrate liquid nitrogen powered engine based on open Rankine thermodynamic cycle using modified air-cooled, single cylinder, four-stroke cycle engine as an expansion engine. The LN2 evaporative system using monochlorodifluoromethane refrigerant heat exchanger and a high-pressure LN2 storage vessel have been designed for this purpose. The engine has been operated with LN2 and measurement of idle speed for different injection pressure at various mass flow rates is carried out. This concept has been focused for some lightweight prime mover applications.

Nomenclature

A	area, m^2
C_p	specific heat, J/kgK
E	modulus of elasticity N/m^2
h	specific enthalpy, J/kg
h_x	local heat transfer coefficient W/m^2K
k	thermal conductivity, W/mK
L	length, m
m	mass flow rate, kg/s
n_t	number of tube passes
Nu	Nusselt Number
P	pressure, Pascals
Q	heat transfer rate, W
R	characteristic gas constant J/kgK
R_e	Reynold's number
r	radius, m
T_h	ambient temperature, K
T_c	liquid nitrogen boiling temperature, K
e	emissivity
F_e	emissivity factor
ψ	availability, J/kg
θ	crank angle
σ	Stefan-Boltzman constant, W/m^2K^4

Abbreviations

FCC	face centred cubic
BCC	body centered cubic
HCP	hexagonal closed packed
LN2	liquid nitrogen
LOX	liquid oxygen

Chapter- 1

Introduction

Recently, there has been increasing concern with the amount of pollution produced by Internal Combustion (I.C) engines. Some of the air-polluting gases emitted by petroleum-powered engines are carbon monoxide, hydrocarbons, oxides of nitrogen, suspended particulate matter, smoke, lead oxide, aldehyde, and ketone etc. Apart from this there are some secondary polluting gases like carbon dioxide, and methane.

The air pollution caused by gasoline and diesel engines, is a major health hazard. Carbon monoxide upon entering the respiratory system combines in the lungs with hemoglobin in the blood stream and reduces ability of the hemoglobin to carry oxygen to the body tissues. Hydrocarbon, along with oxides of nitrogen are responsible for photochemical smoke formation. Nitrogendioxide is transformed in the lungs to form nitrosamines, which cause eye and resipiratory irritation also may affect genes of all living creatures. Small particle of smog get accumulate in lungs. Lead in the air can cause liver and kidney damage, gastrointestinal damage. The dissolving of the acidic chemicals into the atmosphere can cause acid rain, which destroys the forests and buildings. Both hydrocarbons and nitrogen oxides can reach high levels in cities and can be converted by sunlight into photosynthesis smog.

To change from current gasoline and diesel combustion engines to other forms of power has two main reasons, to reduce the dependency on fossil fuels and to reduce the environmentally damaging emission from the combustion of fossil fuels. Also there is an increasing public desire to eliminate polluting engines entirely. Auto manufactures are tackling this problem by developing low and zero emission engines.

A heat engine that operates between atmospheric temperature as a heat source and cryogenic temperature as a heat sink called cryogenic heat engine. The Cryogenic Heat Engine powered by Liquid Nitrogen is a zero emission engine concept. It operates on the thermodynamic potential between the ambient temperature and a reservoir of liquid nitrogen. One way to utilize that potential is through an open Rankine cycle. The university of North Texas and the University of Washington independently demonstrated liquid nitrogen as a non-polluting vehicular fuel The liquid nitrogen is drawn from a tank, pumped up to the system pressure, then vaporized and superheated in a two-stage heat exchange system. The resulting high pressure, near-ambient temperature gas is injected into a quasi-isothermal expander, which produces the system's motive work. The low-pressure gas is exhausted back to the atmosphere. Because a zero emission vehicle is required to produce no smog-forming tailpipe or evaporative pollutants, and because nitrogen gas is its only emission, the liquid nitrogen powered engines meets Zero Emission Vehicle requirements.

1.1 Zero Emission and Low emission Vehicles

A change in motor transport is realistically achievable as most vehicles are replaced in every ten years. Some of the low and zero emission vehicles that are being developed or are already on the market are listed below.

1.1.1. Battery-Electric Vehicles

The major problems with electric vehicles are range and recharge time. With the current technology of batteries, the range of electric cars is up to 150 miles. A full recharge currently takes at around two hours. In urban areas, this range is normally not exceeded in one day, so when this recharge can be done over night it does not matter how long it takes. The main problem comes when on long journeys, stopping on the motorway and waiting for the car to recharge is not practical. Further practical problems can occur when recharging an electric vehicle. People in urban areas own many of the electric cars that are currently

used, but many of their houses do not have garages. This presents problems in getting power cables to cars parked on the side of the road, especially when they are not parked outside your own house. The minor advantages of electric vehicles include the quiet drive, smooth ride and the initial relatively quick acceleration when compared to internal combustion vehicles apart from zero pollution.

1.1.2 Solar-Electric Vehicles

Solar-electric is sometimes said to be the only true way to have a zero emission vehicle. These cars are not charged from the mains, there only power source is the sun. Other advantages include there being less noise pollution than internal combustion engines, and there being no fuel costs. Currently the disadvantages make the solar car impractical. These include existing solar panels being expensive, inefficient and the cars being reliant on the sunshine (which limits its use to particular climates). The Honda 'Dream' Solar Car is currently the holder of the World Solar Challenge race record.

1.1.3 Hybrid-Electric Vehicles

Hybrid electric vehicles (HEVs) are powered in two ways; an engine which can run on petrol, diesel, LPG or other alternative fuels, and a battery. With current technology, electric cars are only useful for short low speed journeys, typically in urban areas. HEVs where designed using the advantages of both internal combustion and electric vehicles to produce a more fuel efficient, cleaner car. The idea for the HEV is to be able to run the engine most efficiently, it is not used at low speeds, it never idles and when it is used it is started instantly by the electric motor. As the battery can provide extra power when needed, the engine can be designed for running at the average load, instead of peak load. This reduces the size of the required engine so gives a significant saving on weight

As HEVs still have an engine, they are only reduced emission vehicles, not zero emission. HEVs were designed as an intermediate step from internal

combustion vehicles to electric vehicles, but the final step towards practical electric vehicles will only be taken if the battery electric technology improves significantly.

1.1.4 Fuel Cell Vehicles

Fuel cells were first used in 1839, but until the resent search for low emission vehicles, this technology has not been properly explored. A fuel cell converts the energy of the fuel into electricity and heat. This is through a chemical process instead of a combustion process like conventional engines. Fuel cells consist of two electrodes: an anode, where the hydrogen fuel is fed in; and a cathode, where the oxygen or air is fed in. The hydrogen splits into hydrogen ions and electrons. The ions flow through the polymer electrolyte membrane and the electrons flow round the circuit forming the current. They both join together with the oxygen at the cathode to produce water.

The fuel cell's emissions being pollutant free, they are also extremely quiet and produce very little vibrations. The main problems are storage of this gas is either as a compressed gas in a high-pressure tank, or as low temperature and pressure liquid hydrogen in an insulated tank.

1.1.5 Gaseous Fuel Vehicles

LPG and CNG are the most commonly used fuels in modern automotive vehicles. LPG is a liquid mixture; normally containing 90% propane, 2.5% butane and higher hydrocarbons, and the rest is a balance of ethane and propylene. It is a by-product of natural gas processing or petroleum refining. At room temperature it is a gas, but is stored in cars as a liquid. There are significant reductions in emissions of LPG vehicles when compared to petrol and diesel vehicles. CNG is a variable gaeous alternative fuel in view of obtaining low exhaust emmisons from I.C.engines. This folows from physicochemical properties of methane; high octane number, wide flammability range, capability to form homogeneous air fuel mixture, low photochemical reactivity, lower global

toxicity of exhaust gases. As an LPG and CNG engine is similar to a petrol engine, vehicles can easily be converted to run on LPG and CNG.

1.2 Overview Of Liquid Nitrogen Powered Prime Mover

There are many thermodynamic cycles available for utilizing the thermal potential of liquid nitrogen. These range from the Brayton cycle, to using two- and even three-fluid topping cycles, to employing a hydrocarbon-fueled boiler for superheating beyond atmospheric temperatures. The easiest to implement is an open Rankine cycle. The principle of LN2 cryogenic engine based on open Rankine cycle is shown Fig 1.1. It begins with a tank of liquid nitrogen stored at 77 K and 1 bar. The nitrogen is pumped, as a liquid, to the system's working pressure. This high-pressure liquid flows into the economizer. The economizer is a shell-and-tube heat exchanger where the shell-side fluid is the exhaust from the expander. While this step is not necessary from an energy point of view, it does have the advantage of providing a frost-free pre-heat to the incoming liquid. Once through the economizer, the vaporized nitrogen enters the heat exchanger, which has a multi-element, tube-in-cross flow configuration. The exterior fluid is the ambient air, which is drawn through the core of the heat exchanger either by the motion of the vehicle or by a fan, depending on the operating regime. This heat exchanger must be able to operate across most of the spectrum of environmental and operating conditions without suffering from the adverse effects of frost buildup. Upon leaving the heat exchanger, the working fluid is a high pressure, near-ambient temperature gas. It is injected into the expander, which provides the motive work for the system. This can be either a positive displacement or turbine engine. Following expansion, the low-pressure exhaust is warm enough to be used in an economizer, where it preheats the incoming liquid, before finally being vented to the atmosphere.

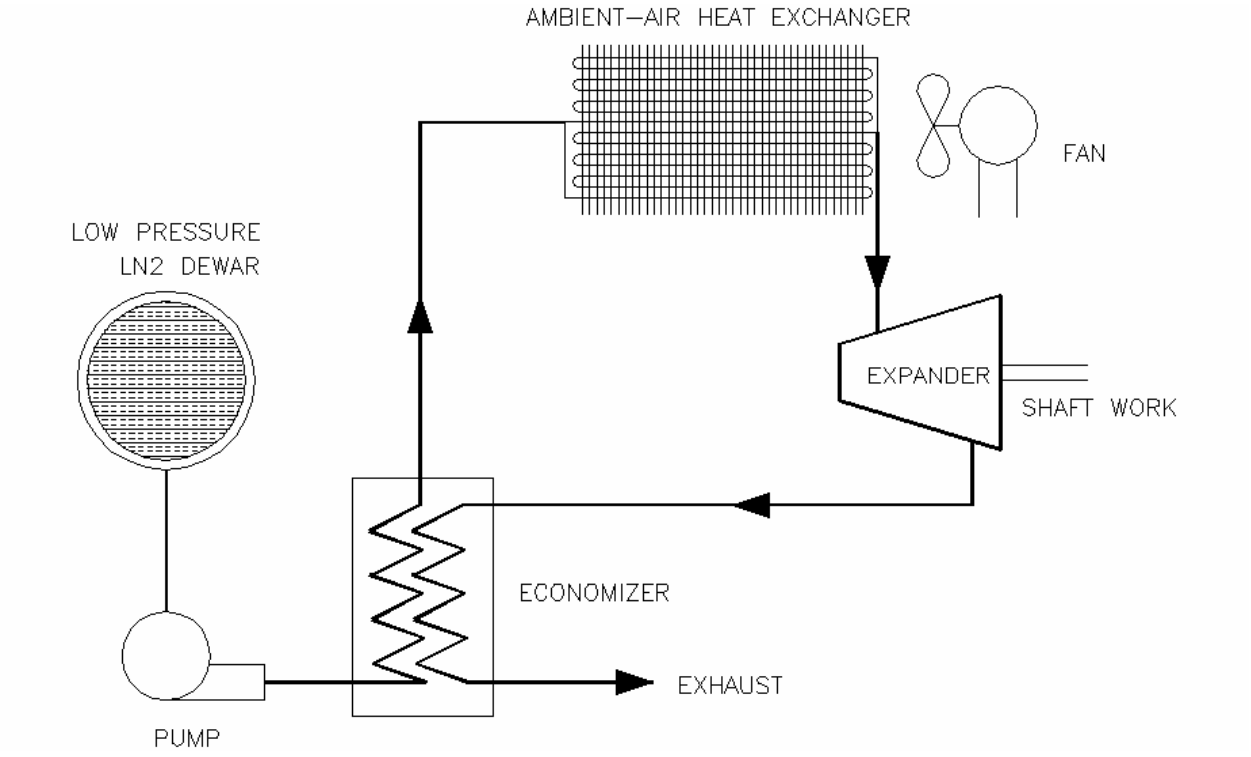

Fig 1.1 Principle of Liquid Nitrogen Cryogenic Engine

1.3 Objective

The main objective of this dissertation is to develop and demonstrate liquid nitrogen powered prime mover using modified four-stroke internal combustion engine as an expansion engine.

Chapter - 2

Literature Review

2.1 Rotary Type Air Motor

A typical vane type air motor is shown in Fig 2.1. This particular motor provides rotation in only one direction. The rotating element is a slotted rotor, which is mounted on a drive shaft. Each slot of the rotor is fitted with a freely sliding rectangular vane. The rotor and vanes are enclosed in the housing, the inner surface of which is offset from the drive shaft axis. When the rotor is in motion, the vane tends to slide outward due to centrifugal force. The shape of the rotor housing limits the distance the vanes slide. This motor operates on the principle of differential areas. When compressed air is directed into the inlet port, its pressure is exerted equally in all directions. Since area A is greater than area B, the rotor will turn counter clockwise. The pressure energy of the compressed air is thus converted into kinetic energy in the form of rotary motion and force. The air at reduced pressure is exhausted to the atmosphere. The shaft of the motor is connected to the unit to be actuated.

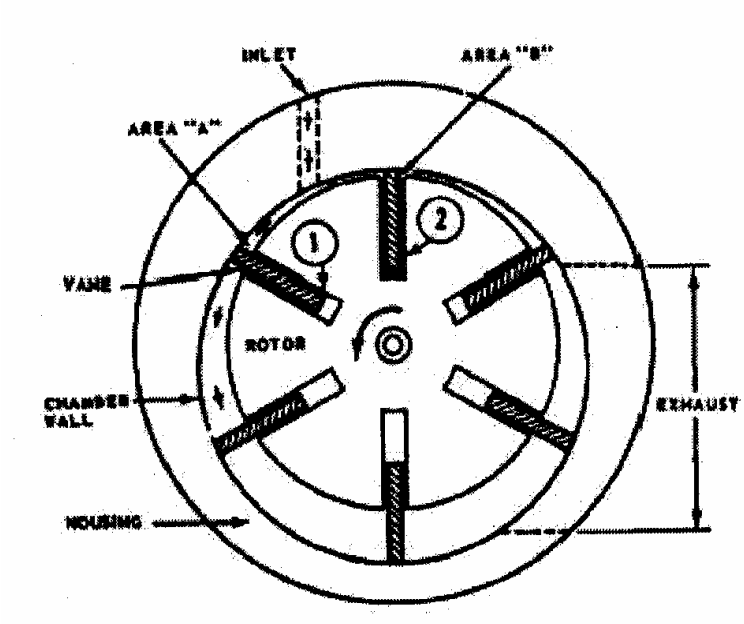

Fig 2.1 Vane Type Air Motor

2.2 Piston Type Air Motor

The radial-piston operates in reverse of the radial-piston pump. The operation of the radial piston motor is shown in the Fig 2.2. This motor is shown with three pistons for the simplicity. Normally it contains seven or nine pistons. When compressed air is supplied into the cylinder bore containing piston 1, the piston moves outward, this cause the cylinder to rotate in a clockwise direction. As the force acting on piston 1 causes the cylinder block to rotate, piston 2 rotate and approach the position of piston 3. As the piston 2 rotates, it is forced inward and in turn forces the expanded gas out of cylinder. Reversing the flow of fluid to it changes the direction of rotation of the motor. This is used in cranes, winches and power transmitting unit in electro hydraulic steering engines.

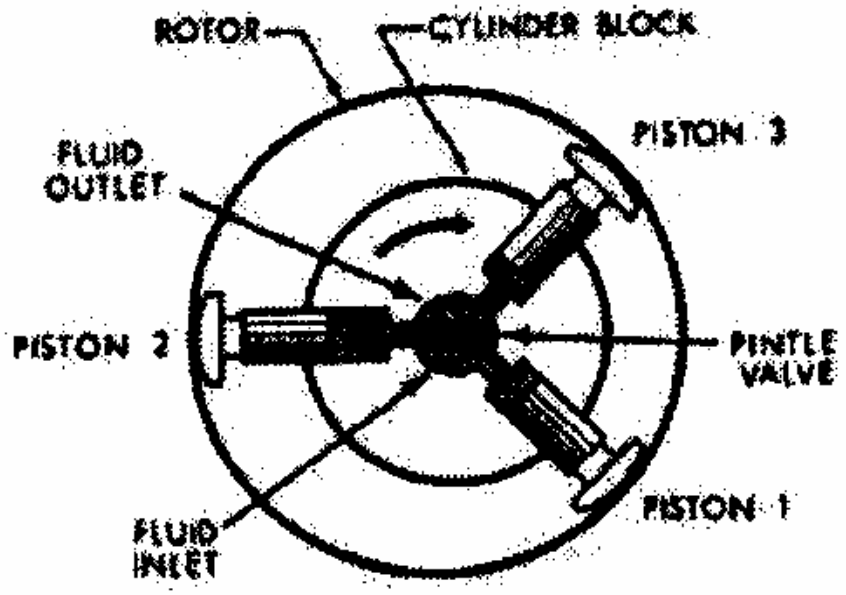

Fig 2.2 Radial piston type air motor

2.3 Liquid nitrogen vehicle by North Texas University

The University of North Texas has designed and built a CooLN2 car running on liquid nitrogen. This is based on cryogenic heat engine concept; the most in intriguing aspect of this concept is the fuel used by cryogenic heat engine powered vehicle can be either liquefied air or liquid nitrogen. The Gas flow diagram of the nitrogen engine by UNT is shown in the Fig 2.3. It consist of three principle components as 1) pressurized tank to store liquid nitrogen, 2) A heat exchanger that heats liquid nitrogen to form nitrogen gas, 3) A pneumatic motor along with Volkswagen transmission that runs the car.

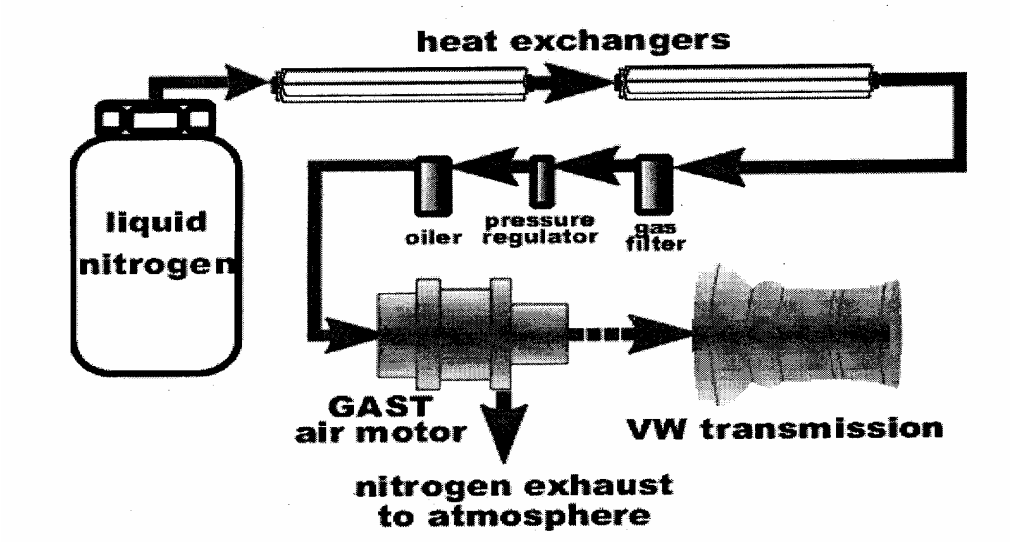

Fig 2.3 Gas flow diagram of nitrogen engine

2.4 Liquid Nitrogen vehicle by University of Washington

The LN2000 is an operating proof-of-concept test vehicle, a converted 1984 Grumman-Olson Kubvan mail delivery van. The engine, a radial five-cylinder 15-hp air motor, drives the front wheels through a five-speed manual Volkswagen transmission. The liquid nitrogen is stored in a thermos-like stainless steel tank, or dewar, that is so well insulated that the nitrogen will stay as liquid for weeks. At present the tank is pressurized with gaseous nitrogen to develop system pressure but a cryogenic liquid pump will be used for this purpose in the

future. A preheated, called an economizer, uses left over heat in the engine's exhaust to preheat the liquid nitrogen before it enters the heat exchanger. Two fans at the rear of the van draw air through the heat exchanger to enhance the transfer of ambient heat to the liquid nitrogen. The air motor is a piston type having a 5-cylinder radial design. Its maximum power output is 15 hp. This air motor is heavy and has very low efficiency because it has a low expansion ratio to avoid moisture condensation when used with ordinary compressed air. Fig 2.4 shows the schematic of the LN2000 car by UW

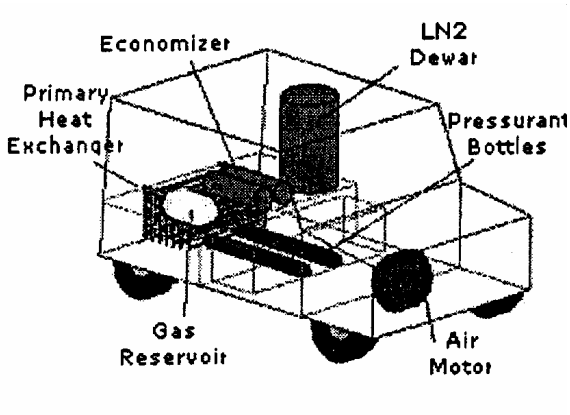

Fig 2.4 Schematic LN2000 car by University of Washington

Chapter - 3

Liquid Nitrogen As A Non-Polluting Fuel

3.1 Properties Of Liquid Nitrogen and Carnot Efficiency

The atmospheric consist 78% of nitrogen gas. By separating nitrogen gas form air, LN2 is produced and now days it is a by-product of liquid oxygen producing tonnage capacity plants.

Boiling Point	77.348 K @ 1 atm
Critical point Temperature	126.19 K @ 1 atm
Critical Point Pressure	33.534 atm
Latent Heat of Vaporization	198.3 kJ/kg @ 1 atm
Sensible heat (sat. vapor at 300K)	234 kJ/kg
Density of Liquid	808 kg/m^3

The efficiency of any heat engine is limited by the Carnot efficiency, is given by

$$\eta = W/Q = 1-(T_C/T_H) \qquad (3.1)$$

where, T_H is source temperature (~300K) and T_L is sink temperature (~80K). The ideal thermal efficiency of 73 % is sufficiently high enough to realize a practical heat engine concept. (Ref; appendix “D” properties of LN2)

3.2 Cryogenic Heat Engine

A cryogenic heat engine is a concept of using a cryogenic substance to produce useful energy. Use of a refrigerator to transfer heat from a thermal reservoir to the atmosphere can be considered equivalent to an energy storage process. To produce useful energy, the heat engine such as a Stirling engine can be operated using the cryogenic thermal reservoir as the heat sink and the atmosphere as the heat resource. A heat engine that operates employing a sub atmospheric temperature thermal reservoir such as liquid nitrogen as the heat sink has been called as cryogenic heat (C-H) engine. A C-H engine may be considered equivalent to a refrigerator operated in reverse. In contrast, a

conventional heat engine that operates using a thermal reservoir that has the temperature higher than atmospheric temperature is considered equivalent to a heat pump operated in reverse.

3.3 Specific Energy level of liquid nitrogen and comparison with battery energy

Comparisons of specific energy provide only a partial view of how a liquid nitrogen powered prime mover can be accepted by the public. The reversible work that can be realized by a chemically inert substance stored at temperature T_l and pressure P_l in an environment T_a is equal to its availability in steady state energy low process

$$\psi = h_l - h_a - T_a (S_l - S_a)$$

where S is entropy. (3.2)

The availability of several cryogen of interest and that of compressed air stored at 20 MPa are shown in table 3.1. It can be seen that the availability of LN2 is approximately 3 times that of compressed air and more than 5 times greater than the specific energy of Pb acid battery (40 kW-hr/kg). In the case of compressed air storage at 20 MPa, the available energy density is so low that, even with an ideal isothermal expansion engine, there is not sufficient space in automobiles to provide comparable driving range.

The specific energy of the on board battery pack in the GM EV1electric vehicle was 110 kJ/kg. The ideal (Carnot) specific work available by the using the heat of vaporization of liquid nitrogen as a heat sink is w= L $[(T_h-T_c)-1]$. For liquid nitrogen under atmospheric pressure, its heat of vaporization is L=200 kJ/kg and its boiling point temperature is T_c= 77K. With atmospheric air at T_h=300K serving as the heat source, the carnot specific work is w=570kJ/kg of liquid nitrogen consumed. For an actual system to achieve, say 110 kJ/kg, it would need to operate 19 % of the carnot value. This should be readily possible, especially considering that the heat source and the heat sink are at constant temperatures

Fluid	Storage Temp (K)	Density (kg/m^3)	Ψ (kJ/kg)	Ψ (W-hr/kg)	Ψ (W-hr/l)
N_2	77.4	809	768	213	173
Air	78.9	886	737	205	181
O_2	90.2	1140	635	176	201
CH_4	111.6	423	1093	304	128
C_2H_6	184.6	545	352	97.7	53.2
Compressed Air	300	233	258	71.5	16.7

Table 3.1

3.4 Possible Thermal Cycles

There are number of possible thermal cycles that can be used for cryogenic heat engine. For using liquid nitrogen as the thermal reservoir, one possibility is to use the nitrogen itself as the working fluid of the heat engine. It is also possible for the working fluid of a cryogenic heat engine to be separate from the nitrogen used as a thermal reservoir. The possibilities include gas cycles (Brayton) and the vapor cycles (Rankine). The cycles can be closed or open, with or without regeneration, can be converted to mechanical energy using a suitable expander.

3.4.1 Open Rankine Cycle

The temperature-entropy diagram for the open Rankine cycle, operated at critical pressure, is shown in Fig 3.1 Labels 1-2 indicates the pumping process. Because pressurization is occurring in the liquid phase of the fluid, the work required is small in comparison with the available work. Process 2-3 is the pass through the economizer and heat exchanger. Process 3-4 and 3-4' are the isothermal and adiabatic modes of expansion, respectively. If the shaded area

represents the available specific work in the cycle, then these two processes provide the upper and lower limits to the expander's performance. Process 4-1 (or 4'-1) is the liquefaction stage. This occurs remotely at an air processing tonnage plant.

The process considered is the expansion of nitrogen gas at 300K and 34 MPa to near atmospheric pressure. The reason the gas expansion stopped above atmospheric pressure is that the dry nitrogen gas can be usefully reheated to prevent frost formation that interferes with heat transfer from the atmosphere. The pressures can be from 20 to 50 kPa. The first process considered is isothermal expansion from 34 MPa to 120 kPa and the work can be easily

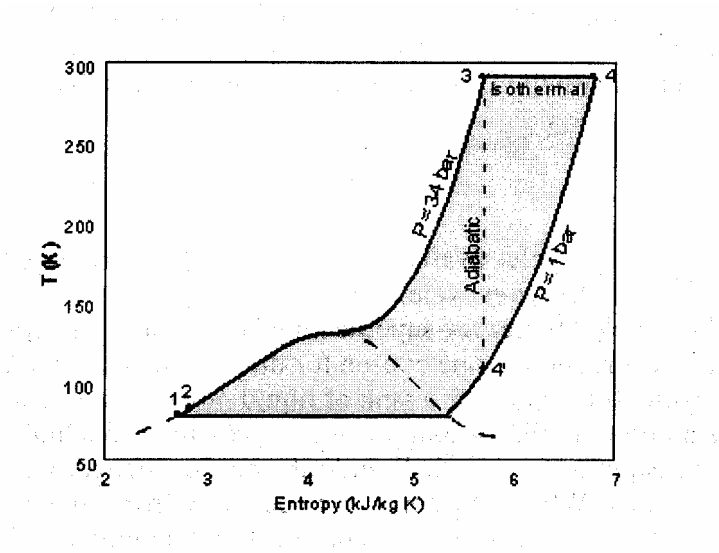

Fig 3.1 T-S diagram of open Rankine cycle

Computed from following equation;

$$w_{isothermal} = R\ T \ln (P_2/P_1) \qquad (3.3)$$

Where R=0.2968 kJ/kg K for nitrogen gas and T=300 K

The result for nitrogen is 292 kJ/kg. Another limiting process is the simple adiabatic expansion of the gas, which no heat is admitted during the expansion. The work available from this process is calculated by using

$$w_{adiabatic} = R\,T\{1-(P_2/P_1)^{(k-1)/k}\}/(k-1) \quad (3.4)$$

Where T=300 K and k=1.4, the ratio of specific heats for nitrogen.
The resulting w adiabatic is 130 kJ/kg of nitrogen exhausted at 150 kPa. These two value set the limits between which we can expect all calculations of energy available from expansion process that use constant pressure reheat between stages.

The model consisting of three expansion stages with two-reheat process is studied. After each stage of expansion, the gas is reheated to 295 K, then injected into the next stage. The expansion ratio for each stage is assumed as 3 with constant pressure reheating between stages. Calculated value for each stage and the work available from expansion is shown in table 3.2.

Station	***Press.,***	***T***	***Enthalpy***
	(kPa)	K	kJ/kg
Initial	3300	300	311.5
Exp.1	1094	219	227.2
Reheat.1	1094	295	306.3
Exp.2	363.4	215	223.6
Reheat.2	363.4	295	306.3
Exp.3	120.6	215	223.5

Table 3.2

$$W = (h_{initial} - h_{exp1}) + (h_{reheat1} - h_{exp2}) + (h_{reheat2} - h_{exp3}) \quad (3.5)$$

$$= 84.2+82.7+82.8 = 249.7 \text{ kJ/kg}$$

Adding additional reheat and expansion may not worth to do, because it increases complexity and pressure associated with additional equipment to obtain the relatively small increases in performance.

3.4.2 Closed Brayton Cycle

Operation of a liquid nitrogen fueled, regenerative, closed Brayton cycle cryogenic heat engine is illustrated in Figure 3.2. The cycle followed by the working fluid, which remains in a gas phase, is (1) a temperature reduction by means of a heat exchange with liquid nitrogen; (2) a compression; (3) a temperature increase by means of a heat exchange with counter flowing gas;(4) a temperature increase by means of a heat exchange with atmospheric air; (5) an expansion; and (6) a temperature reduction by means of a heat exchange with counter-flowing gas.

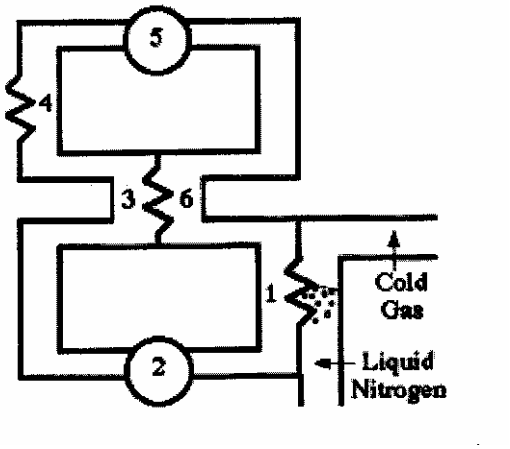

Fig 3.2 Closed Brayton cycle cryogenic heat engine

Considering an adiabatic expander and compressor, the specific energy provided by system is given by

$$w = e_g\, u\, (e_e\, w_e - w_c/e_c) \qquad (3.6)$$

Here,

$$u = A\, \alpha\, L / [R\, T_{cold}\, (p^{\alpha}-1)] \qquad (3.7)$$

u - is the ratio of the working fluid mass flow rate to the liquid nitrogen vaporization rate, T_C = 77K, p is the ratio of the absolute pressures on the high and low pressure sides, A is the working fluid molecular mass (e.g A= 4 kg/kmol for helium), R=8314 J/kmol-K is the universal gas constant, and α=1-1/γ,

where γ is the working fluid's ratio of specific heat capacities at constant pressure and constant volume. For a monatomic gas γ=2/5. Inefficiencies are taken into account by incorporating three terms. e_e and e_c are the efficiencies of adiabatic expander, e_g takes into account all other inefficiencies including those associated with operation of the heat exchangers.

The ideal specific energy provided by adiabatic expander is

$$w_e = R\, T_H\, (1 - p^{-\alpha})/(A\alpha) \qquad (3.8)$$

Where T_H = 300 K. The ideal work that must be done by an adiabatic compressor per unit mass of gas is

$$w_c = R\, T_{cold}\, (p^{\alpha} - 1)/(A\alpha) \qquad (3.9)$$

This equation is derived from equation (3.8) by considering that the initial and final temperatures of a gas that undergoes a reversible adiabatic expansion are related by $T_{hot}/T_{cold} = p^{\alpha}$. Combining equations (3.6) - (3.9) gives

$$w = e_g\, L\{e_e\, p^{\alpha}(\, T_{hot}/T_{cold}) - (1/e_c)\} \qquad (3.10)$$

By way of example, equation (3.10) is used to calculate the specific energy for a system with the values $e_g = e_e = e_c = 0.9$. The specific energy given by equation (3.10) increases with decreasing pressure ratio. Hence, it is desirable to use as small a value for p as possible. It is possible to use a small pressure ratio (e.g., p=3.2 MPa/2.88MPa=1.1) while, at the same time, using a sufficient pressure difference (e.g. 0.32 MPa) to power a vehicle using a high flow rate (e.g. turbine) system. For a monatomic gas working fluid (γ=2/5), and the following values for the rest of the parameters, T_H = 300 K, T_C =77K and L=199 kJ/kg, the specific energy is calculated to be 400 kJ/kg. It should be noted that equation (3.10) only considers the energy available from using liquid nitrogen as a heat sink. The cold nitrogen gas that is produced by vaporizing liquid nitrogen can be used as a heat sink as well.

Chapter - 4

Cryogenic Materials

4.1 Materials For Low Temperature Application

Knowledge of the properties and behavior of materials used in any cryogenic system is essential for proper design considerations. The choice of materials for the construction of cryogenic equipment will be dictated by consideration of mechanical and physical properties such as thermal conductivity, thermal expansively (expansion and contraction cycling between ambient and low temperature) and density (weight of the system relative to its volume). Since properties at low temperatures are significantly different from the those at ambient temperature and there are now several excellent test data compilations given by Mc Clintock and Gibbons, Durham etal & Jonhson

The issue of low temperature embrittlement limits the range of choice in cryogenic design. The purpose of this chapter is show which materials that are ductile at ordinary temperatures retain their ductility at low temperature or liquid nitrogen temperature. Also gives outline about temperature mechanism that governs ductility.

4.2 Low Temperature Ductility

The ability of crystalline materials to deform plastically (ductility) depends primarily upon the mobility of dislocations within the crystal. The mobility of dislocations depends upon temperature, as one might expect and upon several other factors as well. The number of slip system available in crystal influences dislocation mobility. Slip systems are directions within the crystal in which the planes can slip easily over one another. The mobility of dislocation also influenced by impurity atoms at lattice sites, vacancies, interstitial atoms and existence of foreign particles in the crystal.

The number of slip systems is not usually a function of temperature; the ductility of face centered cubic metals is relatively insensitive to decrease in

temperature. Metals of other crystal lattice types tend to become brittle at low temperatures. Crystal structure and ductility are related because the face centered cubic lattices has more slip systems than the other crystal structures. In addition, the slip planes of body centered cubic and hexagonal close packed crystals tend change at low temperature. Which is not the case for face centered cubic metals. Therefore copper, nickel, all of copper nickel alloys and austenitic stainless steel that contain more than approximately 7 % nickel, all face centered cubic remain ductile down to low temperatures, if they are ductile at room temperature. Iron-carbon and low alloy steels, molybdenum and niobium, all BCC, become brittle at low temperature. From this we can understand the response of slip planes and dislocations motion with respect to temperature and its effects on ductility. The generalities summarizing embrittlement at low temperature are shown in the Table 4.1.

Table 4.1 Embrittlement of Structural Material
at low temperature

Remain ductile at low Temperature	*Become Brittle at low Temperature*
Copper	Iron
Nickel	Carbon and low alloy steels
Aluminum and its alloys	Zinc
Austenite S.S containing More than ~7% nickel	Most B.C.C metals
Most F.C.C metals	
Polyterafluoroethylene	

4.3 Low Temperature Strength of Solids

In general, ultimate tensile strength of solid materials is greater at low temperature than it is at ordinary temperatures. This is true for both crystalline and non-crystalline solids and also for many heterogeneous materials as well.

For metals, the strength at 4K may be two to five times that at room temperature. For plastics the strength at 78K may be one and half to eight times greater than the room temperature value. Reduction of the thermal energy of the metal lattice at low temperature is responsible for part of the strength increase of metals. The yield strength of ductile metals increase with decreasing temperature. The yield strength at 20 K is between one and three times the room temperature yield strength for the FCC and hexagonal closed packed metals. A greater tendency towards increase in yield strength at low temperature is shown for BCC metals. In fact for BCC steels, the yield strength increase so rapidly with decreasing temperature that it becomes greater than fracture strength. Thus below certain temperatures these materials fracture before they reach their yield strengths. The yield and ultimate tensile strength of annealed oxygen free copper are shown in Fig 4.1. This figure shows that yield strength of a material can be insensitive to temperature while its tensile strength is increasing by more than a factor of 2. The material has “work hardened” that is, the material hardened itself by generating obstacle to dislocation motion.

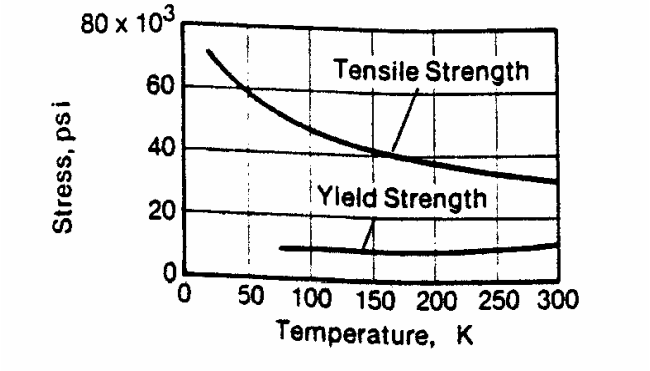

Fig 4.1 Tensile and yield strength of annealed copper

(psi x 6.894×10^{-3}=MPa)

4.4 Thermal properties of Solid

The thermal properties of materials at low temperature of most interest are specific heat, thermal conductivity and thermal expansivity.

Specific heat; Nearly all-physical properties of a solid (e.g specific heat, thermal expansion) depend upon the vibration or motion of the atoms in the solid. The

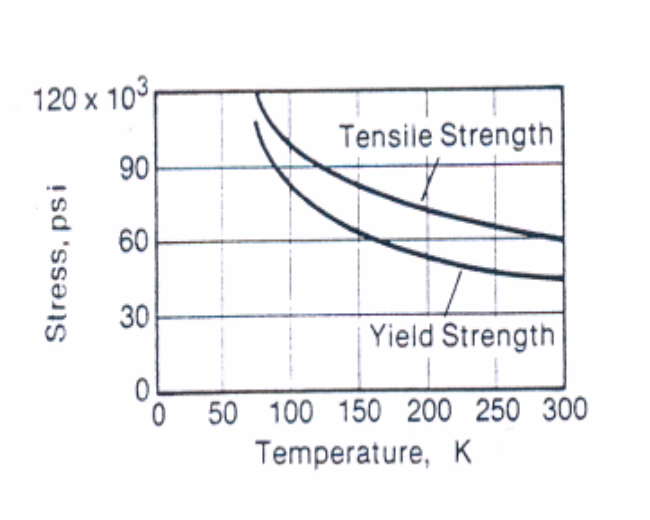

Fig 4.2 Tensile and yield strength plain carbon steel

(psi x 6.894×10^{-3}=MPa)

specific heat at low temperature is important because the variation of specific heat temperature shows how energy is distributed among various energy absorbing modes of the solid. Scientist Debye made a major advance in the theory of heat capacity at low temperature by treating a solid as infinite elastic continuum and considering the excitement of all possible standing waves in the material.

Lattice specific heat, $Cv = 464.5\ (T/\theta)^3 = AT^3$

Where, A is a constant with dimensions of cal/g mol K and T is temperature.
From above equation we see that the lattice contribution to specific heat of solids varies as the third power of the absolute temperature at very low temperatures.
Thermal Conductivity; The thermal conductivity of any material is defined such that the heat transferred per unit time dQ/dt is given by

$$dQ/dt=-k_t\ A(dT/dX)$$

Where, A is the cross sectional area and dT/dX is the thermal gradient.

The temperature dependency of the thermal conductivity of solid is based on three basic energy transport mechanism as 1) Lattice vibration energy transport also known as phonon conduction occurs in all solids-dielectric and metals 2) Energy transport in metals is dominated by electron motion metals of course, also have lattice structure and hence experience a lattice contribution to the thermal conductivity, 3) Molecular motion such as noted in organic solids and gases is another energy transport mechanism. This characteristic disorder as well as the lattice imperfections of organic solids introduces resistance to heat flow. Fig 4.3 shows thermal conductivity curves for different materials.

Thermal expansivity; The mean spacing of the atoms increase with temperature as the temperature of the material increase, thus the coefficient of thermal expansion increases as the temperature increased

Both specific heat and the coefficient of thermal expansion arise from the intermolecular potential and accordingly these two properties are related. This relation is largely due to Gruneisen developed an equation of state for solids based on the lattice dynamic of Debye. He showed that dimensionless ratio γ should be

$$\gamma = \frac{\alpha V}{\beta_T C_v} or \frac{\alpha V}{\beta_S C_v}$$

where, β_T - isothermal volumetric coefficient of thermal expansion, βs - adiabatic volumetric coefficient of thermal expansion

The Gruneisen relation can be expressed in terms of more commonly measured mechanical properties as;

$$\alpha = \frac{\gamma C v \rho}{B}$$

where, ρ - density of material, B – Bulk Modulus, γ - Grunesisen constant, Cv – specific heat

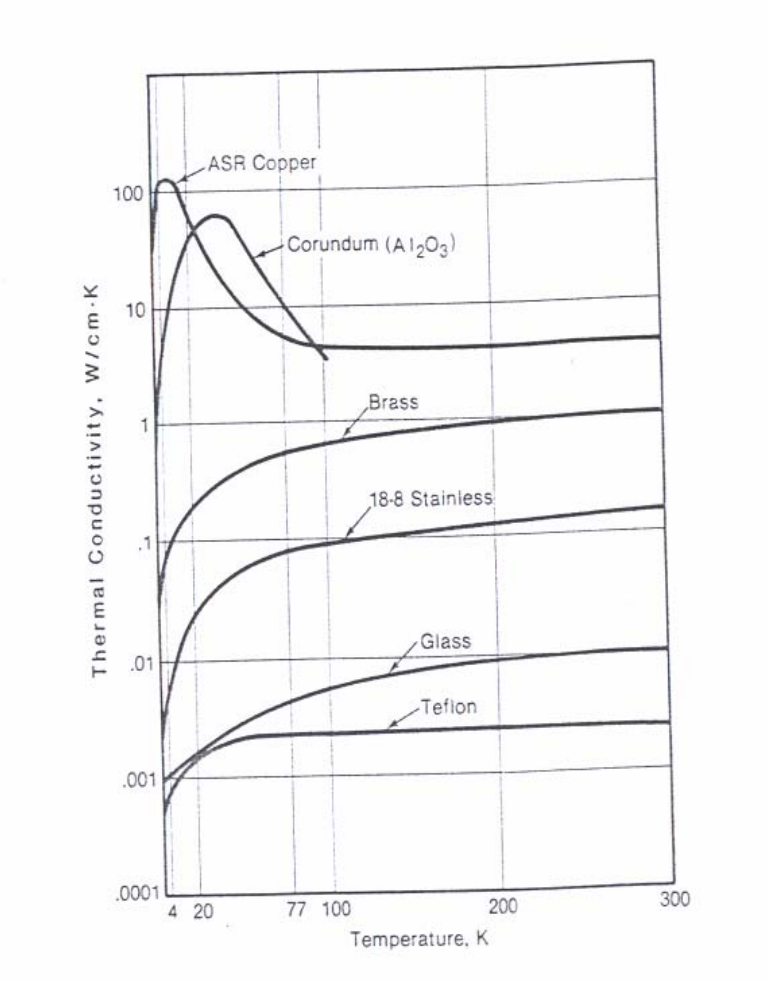

Fig 4.3 Thermal conductivities of different materials at low temperature

4.5 Design consideration

It is convenient to classify metals by their lattice structure for low temperature mechanical properties. The FCC metals and their alloys are most often used in the construction of cryogenic equipment. Al, Cu, Ni, their alloys, and the austenitic stainless steels of 18-8 type are FCC and do not exhibit any impact ductile to brittle transition at low temperatures. As a general rule the structural properties of these metals improve as temperature is reduced. The BCC metals and alloys are usually undesirable for low temperature construction. The HCP metals exhibit structural properties intermediate between those of the

FCC and FCC metals. Plastic also increase in strength as the temperature is decreased but, this is accompanied by a rapid decrease in elongation in a tensile test and a decrease in impact resistance as the temperature lowered.

A cryogenic storage container must be designed to withstand forces resulting from the internal pressure, the weight of the contents, and bending stresses and material compatibility with low temperatures, which has been discussed. Resulting in choosing among FCC metals. Because these materials are more expensive than ordinary carbon steels, a design goal is to make the inner vessel as thin as possible. This constraint also reduces cool down time and the amount of cryogenic liquid required for cool down.

Chapter - 5

Liquid Nitrogen Evaporative system

5.1 Liquid Nitrogen Heat Exchangers*

It is a challenging task for cryogenic engineer to design a heat exchanger system that takes heat from ambient air and vaporizes liquid nitrogen without frost formation. To provide frost free heat to the incoming liquid, the exhaust gas from the engine can passed through a economizer, where it pre-heats the incoming liquid, this heat exchanger (economizer) not necessary in the energy point of view. Then this vaporized nitrogen can passed through a multi-element, tube cross in flow type ambient air heat exchanger. Fig 5.1 shows the components of the LN2 evaporative system with only ambient air heat exchanger.

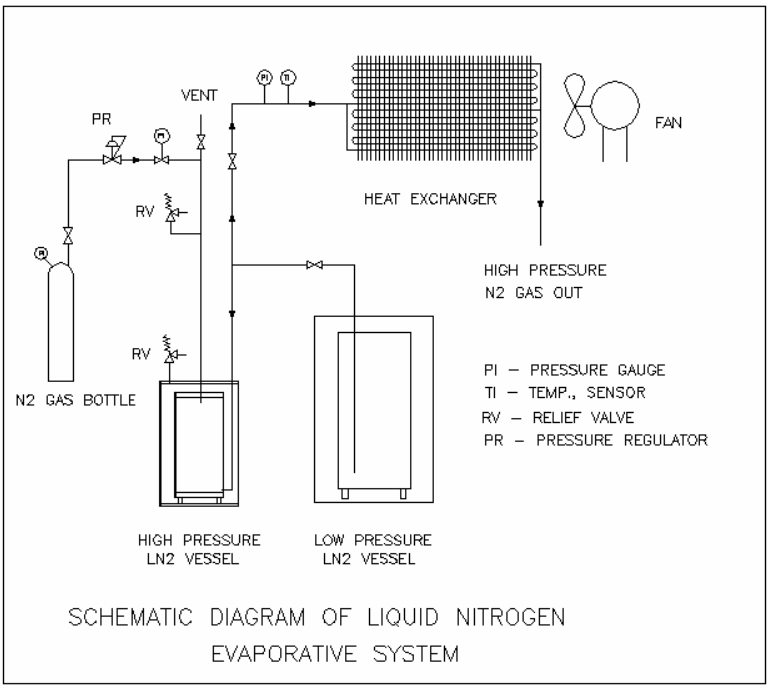

Fig 5.1

(* The details of heat exchanger design, testing and performance for liquid nitrogen evaporative system is discussed in minor project report)

5.2 Economizer:

The economizer is required to vaporize and, if possible, superheat liquid nitrogen. It must not produce excessive pressure drop on either the tube- or shell-side fluids. The economizer must also be safe in both normal operations and during an accident. The tube-side fluid is the incoming liquid nitrogen and the shell-side fluid is the exhaust from the expander.

5.3 Ambient-Air Heat Exchanger

To design a heat exchanger that can operate in a variety of environmental conditions and is structurally robust, while not being hampered by the build-up of frost is not an easy task. There can be more than one approach, but in general, strategies for dealing with frost formation fall into two categories: passive and active control. Passive control involves either preventing frost formation, or over sizing the heat exchanger such that frost build-up is unimportant on time-scales characteristics of engine running. The advantages of passive control are mechanical simplicity and reliability. One disadvantage is that passive systems are, in general, less flexible in dealing with off-design operation.

5.3.1 Design Requirements

To prevent frost buildup on sub ambient heat exchangers, the exterior surfaces must be kept above the freezing point of water. The multi-fluid heat exchange system should be adapted, where heat transferred from source to sink via number of media operating in series. The choice of number of passes is based on two practical considerations. The first is that using an odd number of internal passages allows the inlet and outlet to be at opposite ends of the element, greatly simplifying the manifold. The second is that going to more internal passages such as five or seven, but this can present problems with fabrication, cost and mass. This has to be weighed against the fact that more passes increase the robustness of the system. Robustness ensures that frost-

free performance can be maintained in lower-temperature environments

5.3.2 Mathematical Modeling

The theoretical model is presented to simulate the heat transfer characteristics of the three-pass element. This can help in quickly evaluating changes in geometry and operating environments. For simplicity, some assumptions have been made about the heat exchanger: 1) Steady-state operation. 2) Even flows distribution between and within heat exchanger elements. 3) Zero axial conduction. 4) Zero radiation. 5) Adiabatic corners. 6) Radial symmetry. 7) Single phase (gaseous), fully developed flow. 7) Constant average heat transfer coefficients for each pass.

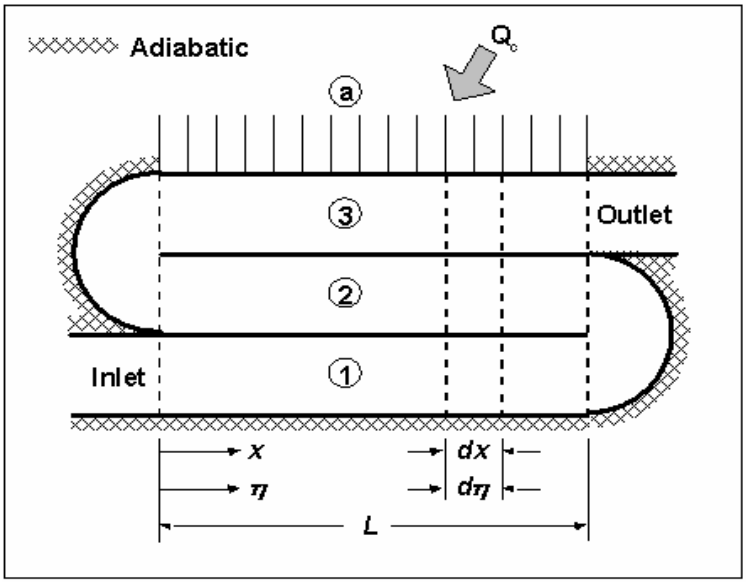

Fig 5.2 Heat exchanger model

These assumptions allow the multi-pass heat exchanger to be modeled as shown in Fig.5.2. In this schematic, η is the non-dimensional span variable, defined as by x/L and Q_c is the heat transfer due to water condensation on the outside surface of the heat exchanger.

Applying the first law of thermodynamics to the differential element dη, the governing equations can be derived for the third, second and first passes as shown in equation 5.1 to 5.3

$$-dQ_c + \dot{m}c_3 dT_3 = p_3 U_{a3}(T_a - T_3)dx - p_2 U_{32}(T_3 - T_2)dx \tag{5.1}$$

$$-\dot{m}c_2 dT_2 = p_2 U_{32}(T_3 - T_2)dx - p_1 U_{21}(T_2 - T_1)dx \tag{5.2}$$

$$\dot{m}c_1 dT_1 = p_1 U_{21}(T_2 - T_1)dx \tag{5.3}$$

Where P_i is the perimeter of the i^{th} tube Ui_{i-1} is the overall heat transfer coefficient between tubes i-1 and i. The governing equations can be non dimensional-ized via the following definitions;

$$\tau_1 \equiv \frac{T_1}{T_a} \qquad \tau_2 \equiv \frac{T_2}{T_a} \qquad \tau_3 \equiv \frac{T_3}{T_a} \tag{5.4}$$

$$K_1 \equiv \frac{P_1 L\overline{U}_{21}}{\dot{m}c_p}\ ,\ K_2 \equiv \frac{P_2 L\overline{U}_{32}}{\dot{m}c_p},\ K_3 \equiv \frac{P_3 L\overline{U}_{a3}}{\dot{m}c_p} \tag{5.5}$$

Q_c is calculated, assuming constant flux F, by

$$Q_c = \int_0^L Fp_3 d\bar{x} = Fp_3 x = Fp_3 Lx \tag{5.6}$$

Which can be non-dimensionalized by

$$K_t \equiv \frac{FP_3 L}{\dot{m}c_p T_a} \tag{5.7}$$

Substituting into the original equation, and writing in matrix notation, gives

$$\begin{Bmatrix} \frac{d\tau_1}{d\eta} \\ \frac{d\tau_2}{d\eta} \\ \frac{d\tau_1}{d\eta} \end{Bmatrix} = \begin{bmatrix} -K_1 & K_1 & 0 \\ -K_1 & K_1+K_2 & -K_1 \\ 0 & K_2 & -(K_2+K_1) \end{bmatrix} \begin{Bmatrix} \tau_1 \\ \tau_2 \\ \tau_1 \end{Bmatrix} + \begin{Bmatrix} 0 \\ 0 \\ K_1+K_a \end{Bmatrix} \quad (5.8)$$

the three boundary conditions for this problem are;

$$\tau_1(0) = \tau_0$$

$$\tau_2(1) = \tau_1(1)$$

$$\tau_3(0) = \tau_2(0) \quad (5.9)$$

the behavior of the heat exchanger is determined entirely by the inlet temperature and the four non dimensional heat transfer coefficients , K_1 , K_2 , K_3 and K_4 . These provide a convenient parameter against which the performance can be optimized to get above freezing wall temperatures. The K_i values are themselves complicated functions of the geometry and heat transfer coefficients, but they provide targets toward which the system design can be adjusted.

5.3.3 Selection of Heat Exchanger for LN2

The design and mathematical model for LN2 evaporative system heat exchanger is discussed in earlier sections. It is very difficult and uneconomical to fabricate a heat exchanger system in short period of time. Hence, a readily available air conditioner heat exchanger with following specification is chosen and tested for LN2 application.

Refrigerant	; MonochlorodifloroMethane
Make	: BSL/Spirotech
Face Area Sq.mtr	: 0.15
Tube Mat. OD & Thickness	: Cu./3/8”/27 Gauge
Number of holes per row	: 15 Nos.

Fin Material and & Thickness : A1, 0.12 mm

Number of fins per cm : 6

Total Face area : 0.13908 m^2

It is being a R22 refrigerant heat exchanger; it is designed to operate at temperature –40.8^o C and the pressure up to 12 bar. The strength of copper increases with decrease in temperature especially below 100 K. Hence, the operating pressure of LN2 prime mover is kept ~ 20 bar This heat exchanger is tested for liquid nitrogen application up to 25 bar pressure. Fig 5.3 shows 3-D picture of a typical cross flow type heat exchanger.

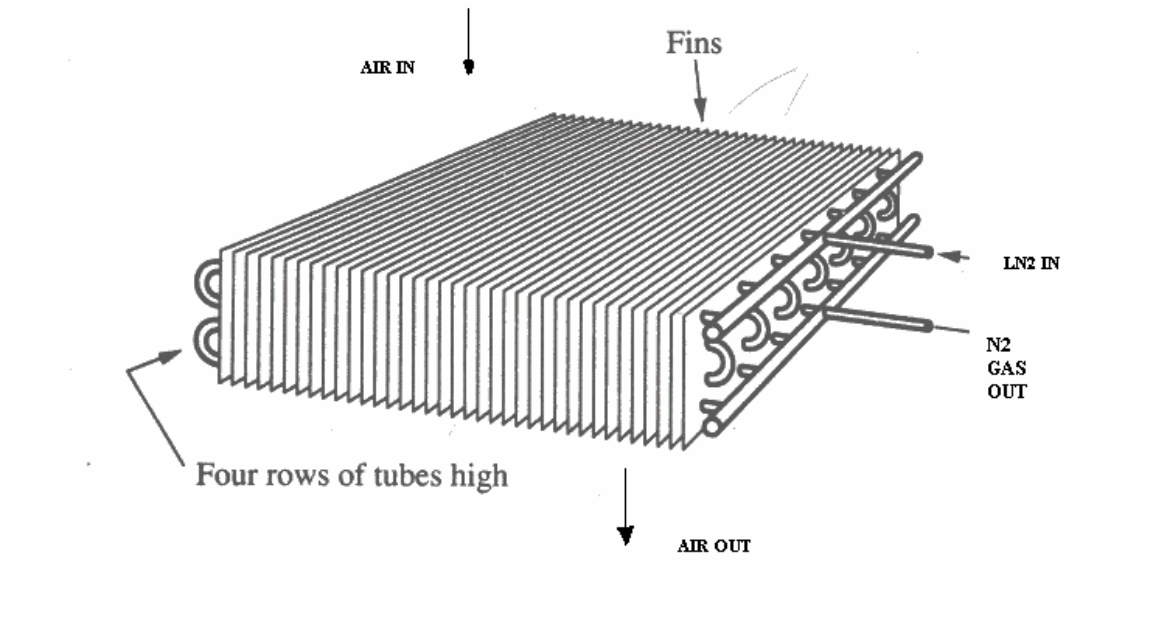

Fig 5.3 3-D picture of typical cross flow type ambient air heat exchanger

5.4 High Pressure Storage Vessel

This liquid nitrogen storage vessel is based on the concept of Dewar design (By James Dewar) a double walled container with the space between the two vessels filled with thermal insulation, air evacuated and maintained under vacuum of 1x10^{-6} torr. The storage vessel consists of an inner vessel, which

encloses LN2 to be kept under pressure. This inner vessel is enclosed by an outer vessel or jacket, which contains the high vacuum necessary to minimize residual gas conduction between inner and outer vessel wall.

The space between two vessels is filled with multi layer insulation by wrapping on inner vessel. The performance of the vessel is highly depends on effectiveness of the insulation. Utmost care was taken while designing this vessel.

This Dewar got two-separate fill and drain lines. The vessel is charged with LN2 with filling line and other one act as vapor venting line. During normal mode of engine operation, one line is pressurized with nitrogen gas and other line is connected to heat exchanger. The LN2 is removed from the vessel by pressurization or using liquid pump. Here, the LN2 is supplied to heat exchanger by pressurization of ullage volume by warm nitrogen gas. Cryogenic storage vessel are not be completely filled. A 10 % ullage volume is provided, so it helps in pressurization.

This vessel is constructed in cylindrical shape with flat ends on both sides Though the flat is not desirable because it requires high thick plates compared to elliptical or hemispherical heads, but the vessel used is a very small capacity, it would be time consuming if we go for elliptical or hemispherical heads.

5.4.1 Inner Vessel Design

The details of conventional cryogenic storage vessel design are covered in ASME Boiler and Pressure Vessel Code VIII. Here, the vessel size is less than 250 liters; Hence, it is not necessary to do design as per ASME code. However to be on the safer side this vessel has been designed as per code. The inner vessel is designed to withstand internal pressure and the weight of the fluid within the vessel and bending stresses and as a result beam bending action. It is constructed with S.S.304, which is best compatible for cryogenic fluid. The thickness of the vessel optimized so that it would take less time for initial cool down of the vessel. According to ASME code the min. thickness of the inner shell for the cylindrical vessel is given by

$$t = \frac{pD}{2S_a\tau_w - 1.2p} = \frac{pD_0}{2S_a\tau_w + 0.8p} \qquad (5.10)$$

Where, p - internal design pressure, D - Inside diameter of shell, D_0 - Outside diameter of shell, S_a =allowable stress (for SS.304 129 MPa), τ_w - Weld efficiency

For the given design pressure of 25 bar, weld efficiency 0.8 (no radiography) and material S.S.304, the inner vessel thickness calculated as **(t) = 2.64 mm** and thickness is kept as 2.8mm

5.4.2 Outer Vessel Design

The outer shell of the dewar has only atmospheric pressure acting on it, and its inner surface is under vacuum, so it would fail due to elastic instability (collapsing or buckling) not because of excessive stress. Failure by elastic instability is covered by ASME code in which design charts are presented for design of cylinders and spheres subjected to external pressure. According to these charts, the vacuum jacket comes under short cylinder category. The collapsing pressure for the short cylinder subjected to external pressure may be calculated from the U.S experimental Model Basic Formula

$$P_a = \frac{2.42 \in (t/D_0)^{5/2}}{(1-v^2)^{3/4}((L/D_0) - 0.45(t/D_0)^{1/2})} \qquad (5.11)$$

Where, L - Distance between stiffing springs for outer shell, D_o – Outer diameter, t – thickness of the shell, ν – poison ration

The collapsing or critical pressure is given by the following expression, according to ASME code is $P_c = 4\ P_a$, The factor 4 is the required safety factor and P_a is allowable external pressure usually atmospheric pressure for the outer shell.

Based on inner vessel dimension, the outer vessel diameter is chosen as D_o = 300 mm, t = 2 mm, ν = 0.29, E = 1.9×10^{11} Pascals. This gives collapsing

pressure as **4.2 bar**, which is 4 times more than the atmospheric pressure, and the thickness chosen is sufficient.

5.4.3 Suspension System Design

One of the critical factors in designing this vessel is to support inner vessel within the outer vessel. Because the poor support system nullify the effect of using high performance insulation. There are three equi-spaced G-10 supports are provided at bottom of the inner vessel, G-10 has very high strength to weight ratio also it is very good insulator. There are six lateral support also provided to avoid shaking of inner vessel and minimize load on tube to tube weld at top of the filling and drain lines.

5.4.4 Safety Device

The operating pressure of the LN2 is kept 20 bar maximum. Also liquid to gas conversion ratio of LN2 is 700 times. So, it is very much essential to have safety precaution while operating this vessel. For this reason there is a safety relief valve provided with vacuum space of the vessel. So, in any case inner burst immediately the safety relief valve opens and discharge all nitrogen gas to atmosphere.

5.4.5 Insulation

There are several types of insulation that can be used in cryogenic equipment. These include 1) Expanded foam, 2) Gas-filled powders and fibrous material 3) Vacuum alone 4) Evacuated powders and fibrous class material 5) Multi layer insulation. In this pressure vessel both multi layer insulation and vacuum together used to minimize conduction, gaseous convection and radiation mode of heat in leak to the inner vessel. Multilayer insulations consist of alternating layers of aluminized Mylar, which is highly reflecting material and low conductivity fiberglass material is used between layers. The vacuum space between two shells essentially eliminates two solid conduction and gaseous

convection. Modified Stefan –Boltzman equivation, gives the radiant heat transfer rate between two surfaces

$$Q^{\cdot} = F_e F_{1-2} \sigma A_1 \left(T_2^4 - T_1^4\right) \qquad (5.12)$$

F_e = Emissivity factor, F_{1-2} = Configuration factor, σ = Stefan – Boltzman constant, A_1 = Area of surface1, T_2 = Temperature of surface 2 in absolute, T_1 = temperature of surface1 in absolute.

The inner vessel is completely enclosed by outer vessel, so $F_{1-2} = 1$, subscript 1-refers inner vessel, 2-refers to outer vessel.

$$\frac{1}{F_e} = \frac{1}{e_1} + \frac{A_1}{A_2}\left(\frac{1}{e_2} - 1\right) \qquad (5.13)$$

e = emissivity of surface, A = Surface Area

Radiant heat transfer can be reduced by interposing floating (thermally isolated) radiation shields of highly reflective material between the hot and cold surfaces. For 'N' shield between the hot and cold surfaces, the emissivity factor for a shield with emissivity e_s is (parallel flat plates).

$$\frac{1}{F_e} = \left(\frac{1}{e_1} + \frac{1}{e_s} - 1\right) + (N-1)\left(\frac{2}{e_s} - 1\right) + \left(\frac{1}{e_2} + \frac{1}{e_s} - 1\right) \qquad (5.14)$$

The vessel is pumped with turbo molecular vacuum pump upto 5x10-6 mPascals. This vacuum retained in the annular space, due to there is no residual gas conduction.

Calculation for emissivity factor and heat in leak to the vessels;

Inner vessel (D=210mm and L=370mm)

Cylindrical surface area = 0.244 m

End plates surface area = 0.0693m^2

Total surface area (A_1) = 0.333 m^2

Outer Vessel (D=300 mm and L=550mm)

Cylindrical surface area = 0.518 m^2

End plates surface area = 0.142m^2

Total surface area (A_2) = 0.66 m^2

Emissivity of $SS(e_1)=0.048$, emissivity of MLI (e_s) = 0.4 and

Number of insulation layers (N)=20

Using equation 5.14 the emissivity factor (F_e) = 0.02317

For T_1 (LN2) =78k, T_2 (atmosphere) =300k, F_e = $9.798*10^{-4}$ and

F_{1-2} =1 (fully enclosed area)

Using eqn.5.12 calculated heat in leak to the vessel (**Q**) is 3.493 watt

LN2 evaporation rate = 0.0776 liter/hr or 1.862 liters/day

Heat in leak due to conduction heat is ignored, fill and drain lines are vacuum jacketed for sufficient length.

5.4.6 Finite Element Analysis for End Plates of Inner and Outer Vessels

The end plates of the inner vessel are subjected to maximum internal design process of 25 bar. The static stress due to this pressure is analyzed with the help of FEA program, and the stress distribution pattern is shown in Fig 5.4. The end plates of the outer vacuum vessel will be subjected to atmospheric pressure acting from outside. As per ASME, it must be designed for 4 times atmospheric pressure i.e., approx. 4 bar, The maximum static pressure induced in the plate is calculated with the help of FEA program and the stress distribution for the same is shown in Fig 5.5. In both the cases the maximum average stresses is kept below the atmospheric pressure. The details of end plates design parameters given in appendix “A”

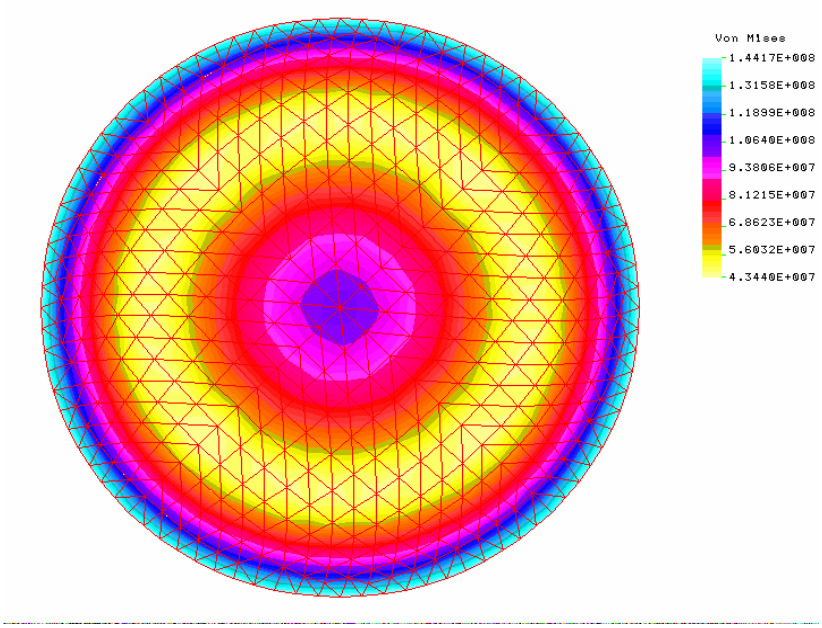

Material S.S.304, thichness:12 mm

Fig 5.4. FEA out put for inner vessel end plate

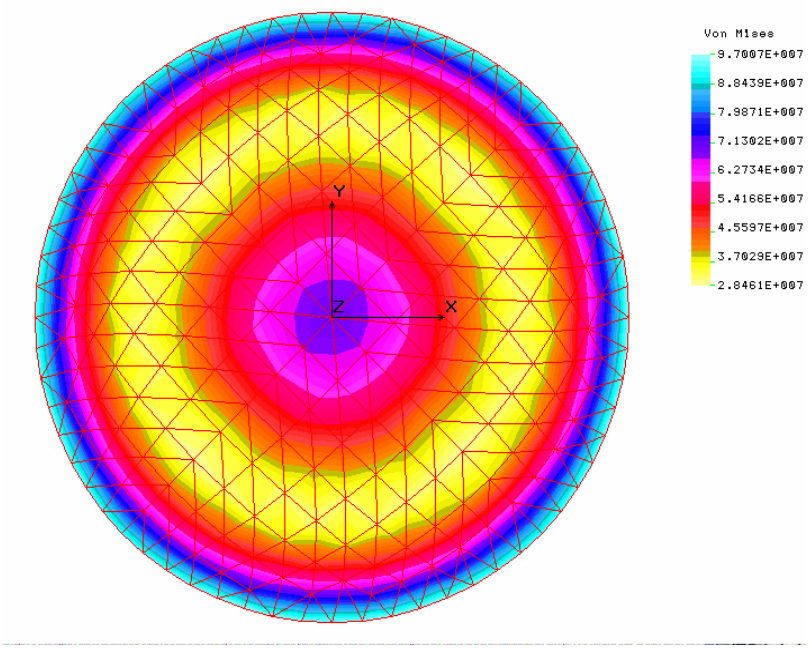

Material S.S.304, thichness:8 mm

Fig 5.5 FEA Output for outer vessel end plates

Chapter - 6

Simulation of Expansion Engine

6.1 Theoretical Analysis of Expander

The thermodynamic simulation of a reciprocating expander is dependent on various engine design and operational parameter. A theoretical model for heat transfer is used in this analysis to predict the effect of injection pressure and temperature on the workout put of expander as a function of bore, stroke and engine speed (RPM). A generalized simulation procedure adopted to examine, the a wide range of piston cylinder head configurations. The details of simulation methodology are discussed in this section.

6.1.1 Reciprocating Engine Model

A transient analysis is applied on the control volume bounded by the piston and cylinder walls as shown in Fig. 6.1

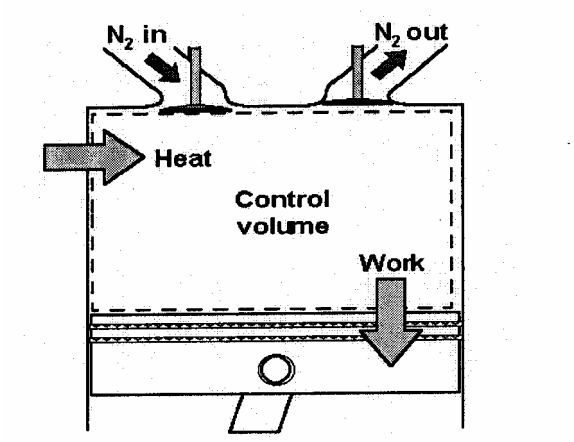

Fig 6.1 Control volume bunded by piston and cylinder

Assumptions;

1. The cylinder content have uniform properties and be governed by the ideal gas equation of state

2. The heat transfer to the gas is coupled with the expansion process once the cut-off point is reached and ceases when the piston reaches bottom dead center (BDC)
3. The surface temperature of all internal surface is assumed to be constant

The instantaneous state of the N2 gas in the control volume is determined from energy conservation and the ideal gas equation of state. The energy equation for the cylinder content is expressed

Steady state energy flow equation for control volume

$$dp/d\theta = (\gamma - 1)/V\{(dQ/d\theta) - \gamma/(\gamma - 1)\, pdV/d\theta + (dm_i/dt)h_i - (dm_e/dt)h_e\} \qquad (6.1)$$

where, p - pressure, θ - crank angle, γ - specific heat ratio, V - volume, Q - heat transfer, dm/dt - mass flow rate, h - enthalpy, subscripts “i”, and “e” refer to injection and exhaust gas properties.

The cylinder volume is obtained from the standard slider-crank relationship as follows;

$$V = V_h + V_c + \pi d^2 S/8(1 - \cos\theta + R - (R^2 - \sin^2\theta)^{1\backslash 2}) \qquad (6.2)$$

d - Cylinder diameter, S - length of stroke, R - ratio of connecting rod to crank radius, V_c - clearance volume (measure of minimum gap between piston and cylinder head), V_h = head volume i.e. volume inside the expansion chamber

The expression for “dv/dp” is obtained by differentiating equation 6.2

6.1.2 Piston cylinder Heat Transfer

It is essential to know the heat transfer rate to N2 gas and its relationship with bore, stroke and revolution. The empirical correlation for average heat transfer coefficient is available for I.C engine. The heat transfer analysis from a engine during motoring test may be close to the expander engine situation and provides useful data for proposed heat transfer model. For the purpose of simplicity the heat transfer from the cylinder walls can be assumed to be similar to turbulent heating of gas in a pipe as follows;

$$Nu_d \approx \mathrm{Re}_d^m \, \mathrm{Pr}^n \quad (6.3)$$

Nu - Nusselt number, Re - Reynold's number, Pr - Prandtle number, m = 0.8 for fully developed flow, n = 0.3 or 0.4 for cooling or heating respectively,

Thermal conductivity and viscosity of the N2 gas is obtained from data tables. From the eqn 6.3, the local heat transfer coefficient is calculated using ;

$$Nu = h_x.d / k \quad (6.4)$$

The rate of heat input to the gas is determined by assuming that h_x applies to all surfaces in the expansion chamber and that the wall temperature T_w is uniform and constant throughout the cycle, corresponding

$$dQ / dt = h_x A_w (T_w - T) \quad (6.5)$$

The total surface area exposed to heat transfer is given by;

$$A_w = A_p + A_h + A_c + \pi dS / 2 \, (1 - \cos\theta + R - (R^2 - \sin^2\theta)^{1\backslash 2}) \quad (6.6)$$

where, h_x - Local heat transfer co-efficient, T_w - uniform wall temperature, A_p - Area of piston face, A_h - internal area of head volume, A_c - surface area of clearance volume

6.2 Standard Otto Power Cycle

Spark ignition, petrol, four stroke engine consist of four processes involving air-fuel mixture intake, compression of charge, power and exhaust stroke. This process for an Otto cycle can be represented in the P-V diagram is shown in Fig 6.2. Engines operating with this power cycle have been highly developed over the years. However, There are fundamental draw back in this engine

1. Back work required to compress air-fuel charge reduces the net work output

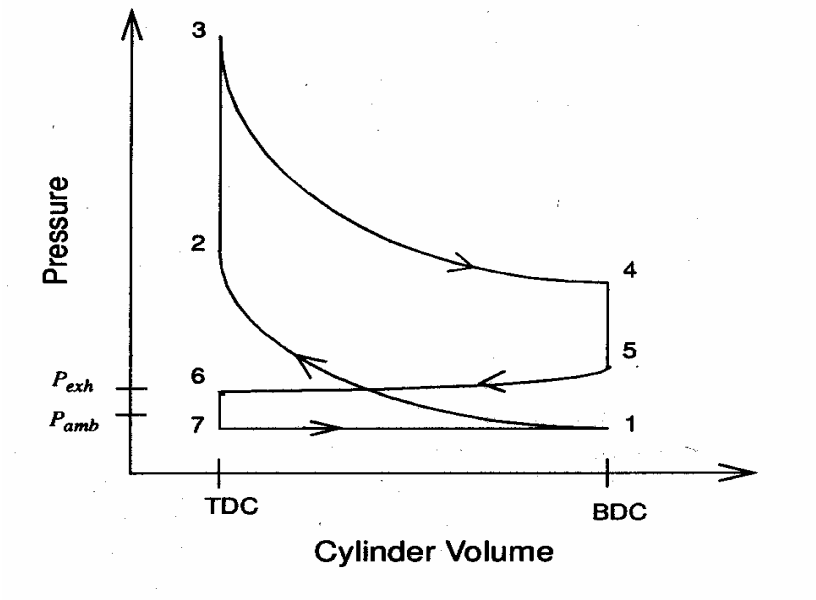

Fig 6.2 p-v diagram of Otto cycle

2. Net work loss due to additional work required to expel the exhaust gasses
3. Un avoidable heat transfer losses

The work done on the piston by the gas during the expansion process between 3 to 4 is

$$W_{\exp} = C_v T_3 (1 - (p_4 / p_3)^{(\gamma-1)/\gamma}) \quad (6.7)$$

The sum of the work of the four strokes equals the network output of the engine per unit mass of working fluid as follows

$$W_{\exp} = W_{\exp} - W_{comp} + W_{\text{int}} - W_{ext} \quad (6.8)$$

6.3 Two Stroke Expansion Cycle

Expansion engines are positive displacement machines where internal energy of the gas is directly converted to the external work owing to the pressure exerted by the gas. The pressure of the gas acts on a piston, which is pushed. This piston is connected to a flywheel through a crank and connecting rod. Like other reciprocating machines, it operates cyclically with opening and losing of valves in synchronization with piston displacement. The flywheel acts to smooth

out the fluctuation of speed. An alternative or other type of load can be connected to get useful work done.

By incorporating the following modification on a four-stroke cycle engine, it can be made to work on two-stroke cycle

1. Speed of the cam is same as that of crank shaft
2. Optimization of valve lift and timing

The components of the engine is to be modified so that there is maximum heat transfer from ambient air to engine to maintain isothermal expansion process through out the expansion stroke. The components also should be verified for the mechanical reliability, maintenance of alignment among mating parts and strength at given expansion ratio.

6.3.1.Selection of Engine

A four stroke cycle I.C. engine with highest possible compression ratio is a best suitable for modification into an two stroke cycle expansion engine, because it can be structurally robust for higher expansion ratio. A four stroke engine with following specifications selected for modification into two-stroke cycle expansion engine based on availability of engine in the market and results of the LN2 evaporative system

Engine specification

Type		: Four stroke, single cylinder, air cooled
Displacement		: 97.2 cc
Bore & Stroke		: 49mmX52mm
Compression ratio		: 9:1
Valve drain		: Chain driven
Intake valve,	Opens	: 0^{o} BTDC (at 1 mm lift)
	Closes	: 25^{o} ABDC (at 1 mm lift)
Exhaust valve,	Opens	: 25^{o} BBDC (at 1 mm lift)
	Closes	: 0^{o} ATDC (at 1 mm lift)

6.4 Real Cycle Analysis

The ideal P-V diagram of the expansion process inside reciprocating expansion engine is shown in Fig 6.3. The real cycle P-V diagram deviate from ideal cycle due to followings;

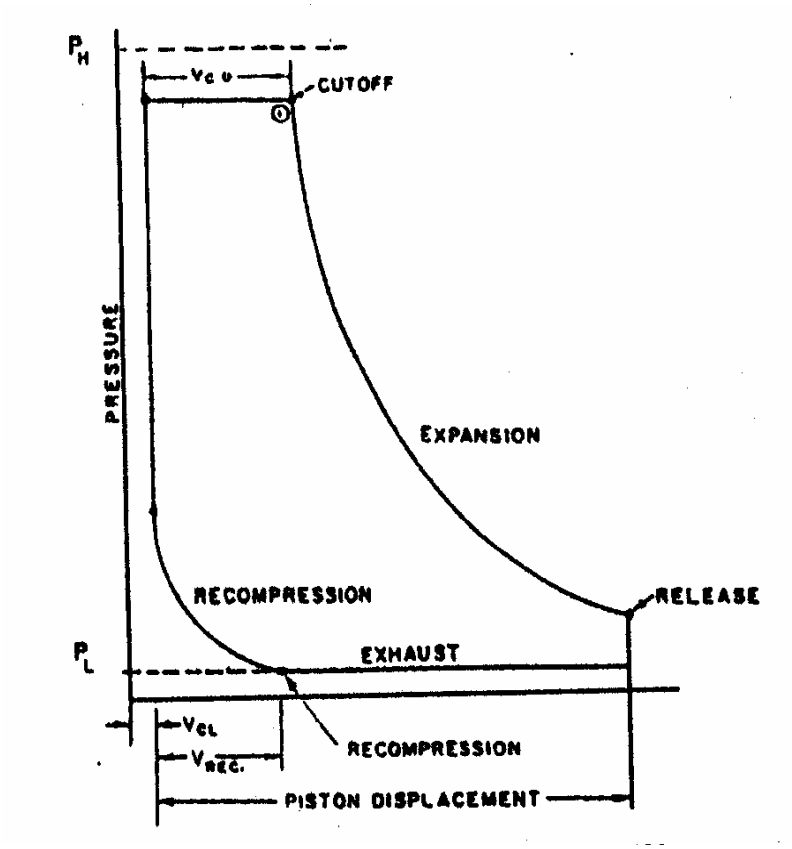

Fig 6.3 Ideal P-V diagram for a typical expansion engine

1. There is pressure drop across valve, conductance and heat exchanges
2 The corners of diagrams are rounded because of finite time of valve closing and opening
3 The expansion process is represented almost flat indicating the departure from the ideal isothermal expansion and thereby causing reduction in efficiency
4 The frictional heating will help in maintaining isothermal process at the cost of power loss

6.5 Effect of Injection pressure on Net Work output

Prior work conducted at university of Washington has indicated that significant gains in the overall efficiency of ambient heated LN2 propulsion system would result if an effective isothermal engine would be developed. Fig 6.3 shows the specific work (using formulae 6.9,6.10& 6.11) plotted as a function of peak cycle pressure, with peak temperature as a parameter, for ideal adiabatic and isothermal expanders

$$w_{isothermal} = R\,T \ln (P_2/P_1) \qquad (6.9)$$

$$w_{adiabatic} = R\,T\{1- (P_2/P_1)^{(k-1)/k}\}/(k-1) \qquad (6.10)$$

$$w_{pump} = v\,(P_2 - P_1) \qquad (6.11)$$

The cut off point for N2 gas injection is adjusted so that the final pressure is always 0.11 Mpa. For the range of injection pressure shown the isothermal work increases monotonically with increasing pressure, where as the adiabatic work is less dependent on peak cycle pressure above 4 bar. The inclusion of pump work result in a specific work maximum for the expansion processes, even though it is not evident in the isothermal work plotted here.

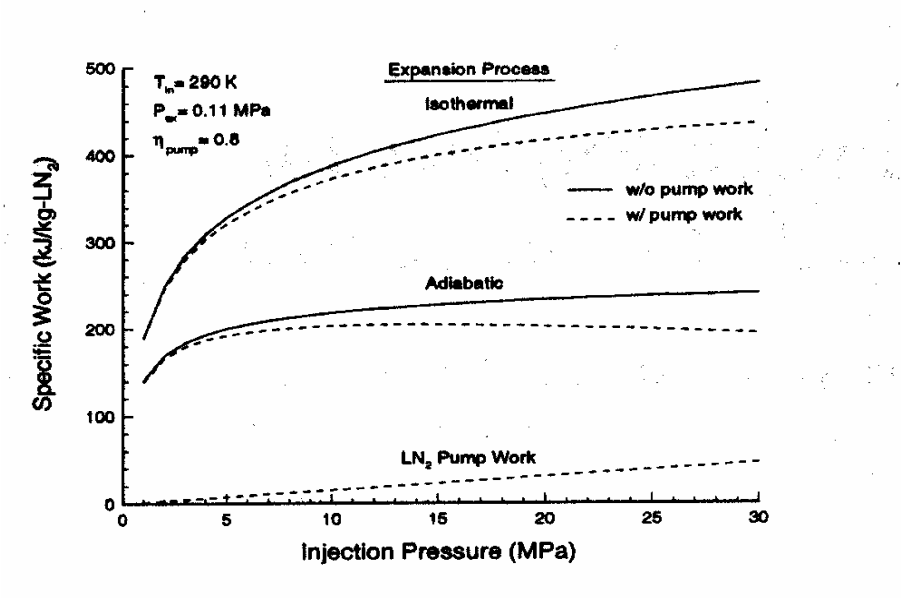

Fig 6.4 Specific work as a function of peak cycle pressure

The cut off point for N2 gas injection is adjusted so that the final pressure is always 0.11 MPa. For the range of injection pressure shown the isothermal work increases monotonically with increasing pressure, where as the adiabatic work is less dependent on peak cycle pressure above 4 bar. The inclusion of pump work result in a specific work maximum for the expansion processes, even though it is not evident in the isothermal work plotted here. From this we can understand that for the maximum specific work the nitrogen gas needs to be used efficiently, the expansion engine required to be operated at higher pressure and the heat transfer is to be maximized during expansion process.

Chapter - 7

Experimental Test Setup

7.1 Conversion of Existing Four-Stroke Cycle Into Two-Stroke Cycle Expansion Engine

A single cylinder, air-cooled, 100 cc four-stroke engine, as discussed in chapter 6 is chosen for this purpose. In four strokes engine the cam speed is half of the crankshaft speed. The drive to the camshaft is transmitted through chain drive mechanism and the entire assembly is covered inside the engine body assembly.

7.1.1 Camshaft Driving Mechanism

The camshaft driving mechanism, oil pump, spark ignition system components have been removed. Equal size sprocket has been mounted on crankshaft and camshaft using adaptors made of mild steel. The crankshaft adaptor is mounted with key slot and key pin. The camshaft adaptor is mounted with the help of bolts and tapped holes already exist on camshaft. The camshaft sprocket connected to crankshaft using chain mechanism. Fig 7.1 shows the photograph of camshaft driving mechanism.

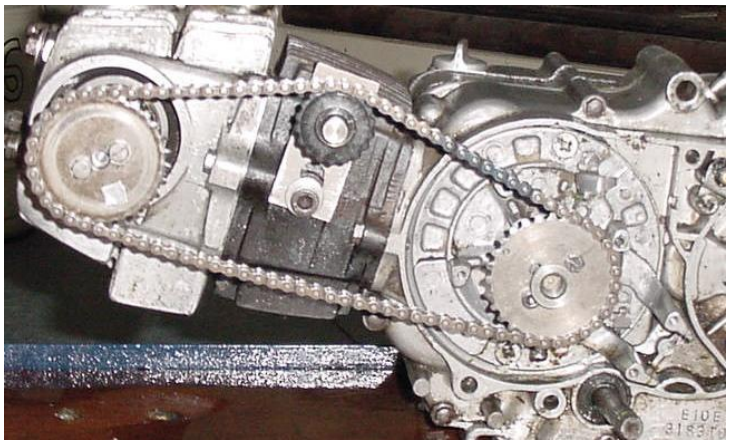

Fig 7.1 Photograph of camshaft driving mechanism

7.2 Test Rig

Fig 7.2 Shows the P&I diagram of the liquid nitrogen powered prime mover experimental test setup. Fig 7.3 photograph of the test rig. The pumping work requirement of Rankine cycle accomplished with the help of high-pressure liquid nitrogen vessel and a high-pressure nitrogen gas cylinder. The major components of the systems as follows

7.2.1 High-pressure liquid nitrogen vessel

This is a super insulated double-jacked vessel designed to operate up to 22 bar pressure. The capacity of the vessel is 12 liters including ullage volume considered for pressurization. This vessel can supply 3.806 g/s nitrogen gas for 45 minutes. This vessel is kept at bottom platform of the rig.

7.2.2 Heat Exchanger

The heat exchanger used for monochlorodifluoromethane refrigerant air conditioner is tested for liquid nitrogen application and used in this experimental setup. It is an ambient air heated cross flow type heat exchanger made up of copper tubes and aluminum fins. Experiments have been carried out to find out maximum possible rate of liquid nitrogen evaporation for the given flow velocity of air over the heat exchanger. This heat exchanger is vertically mounted on the test setup for purpose of convenient, functionally it should be mounted horizontally. A fan of capacity 75 watts is mounted behind this heat exchanger, which is blowing air with the velocity of 3.4 m/s.

7.2.3.Expansion Engine

Fig 7.5 shows photograph of converted four-stroke into two-stroke cycle expansion engine. The high-pressure nitrogen gas from the heat exchanger is injected into this engine, where the gas being expanded and corresponding power obtained from the engine output shaft. The aluminum body

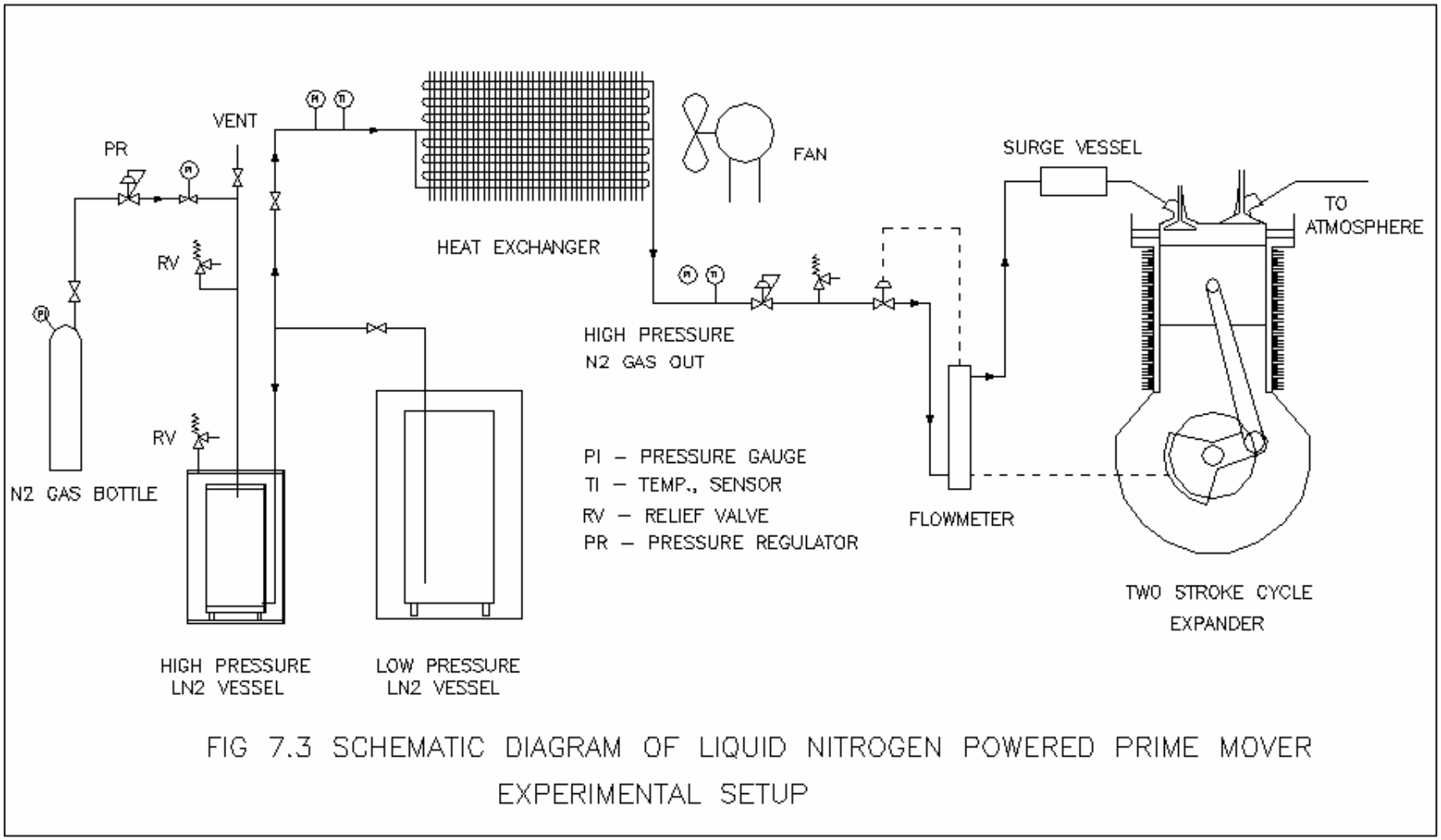

FIG 7.3 SCHEMATIC DIAGRAM OF LIQUID NITROGEN POWERED PRIME MOVER EXPERIMENTAL SETUP

Fig 7.3 Photograph of test rig

of the engine with fins keeps the expansion engine not becoming cold by taking heat from atmospheric air. It is mounted at bottom of the rig so that the engine can be kick started with leg.

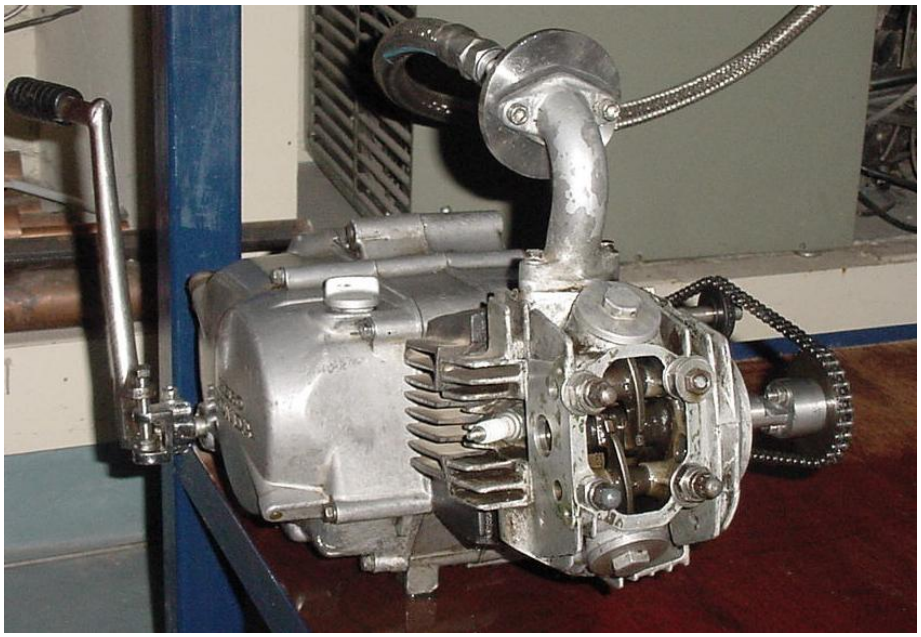

Fig 7.4 Photograph of modified four stroke engine

7.2.4 Flow measurement

There is a rotometer type flow meter, which can measure maximum of 300 LPM has been mounted before supply manifold to the engine. It is having a knob to adjust the flow rate. It can withstand maximum of 22-bar pressure. The pressure drop across the flow rate is very low and is neglected in measurement.

7.2.5 Pressure Measurement

There are two high pressure regulators are placed after N2 gas bottle and before engine suction manifold. With the help of these regulars the LN2 vessel pressure and supply pressure to the engine can be varied. There are two pressure gauges mounted at entrance and exit of the heat exchanger, one at gas

injection point and other one is in the liquid vessel. All the pressures are measured in gauge terms.

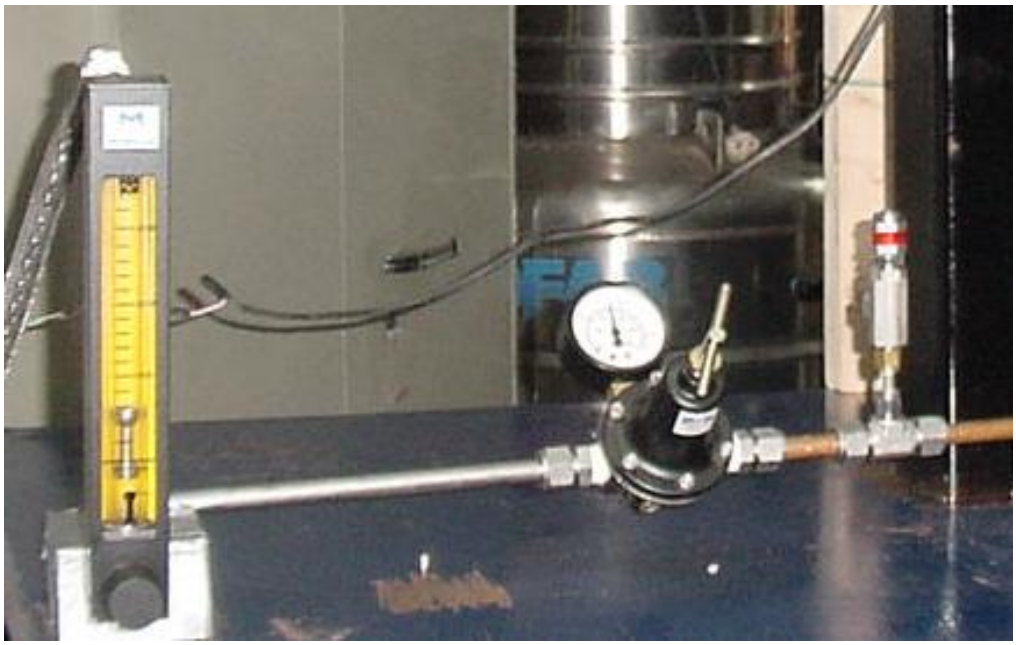

Fig 7.4 photograph showing flowmeter and pressure regulator

7.2.6 Temperature Measurement

It is important to measure temperature at exit of the heat exchanger to avoid cold N2 gas entering to the engine, which will damage the engine operation. The exhaust gas temperature also is one of the important parameter to monitor, if the temperature goes below sub zero which can also damage the engine operation. The entrance temperature to the engine is measured with the help of a diode sensor mounted on the tube wall. The exit temperature of the exhaust gas from the engine is measured with help a portable temperature monitor.

7.2.7 Speed Measurement

There is no brake dynamometer setup made to measure load characteristics of the engine. With the help of pressure regulator and flow meter the injection gas pressure and mass flow meter to the engine is varied. The idle speed variation with respect to different mass flow rate and injection pressure is measured using a non-contact tachometer.

7.3 Engine operation

Initially, the high-pressure vessel filled with liquid nitrogen and ullage volume pressurized with external nitrogen gas cylinder. This high-pressure liquid passes through heat exchanger where, it absorbs heat from atmosphere, resulting high-pressure ambient temperature nitrogen gas injected into expansion engine. The exhaust gas temperature is lower than the ambient temperature.

7.4 Performance of LN2 Engine

The engine crankshaft speed for the various injection pressures at different mass flow rate is measured using a tachometer. The readings are shown in the Table 7.0. There is no load connected to the engine, it is kept running in neutral gear.

Pressur (Mpa)	Mass flow Rate (g/s)			
	0.9516	**1.903**	**2.855**	**3.806**
0.2	700	1560	--	--
0.3	793	1634	--	--
0.4	857	1723	--	--

0.5	1050	1809	2422	--
0.6	1173	1887	2550	2807
0.7	1308	1950	2620	2879
0.8	1397	2078	2699	2912
0.9	1509	2145	2750	2989
1	1606	2197	2800	3275
1.1	1626	2224	2867	3333
1.2	1666	2343	3200	3495
1.3	1690	2398	3298	3789
1.4	--	2452	3768	4168
1.5	--	2489	3867	4234
1.6		2519	--	4322

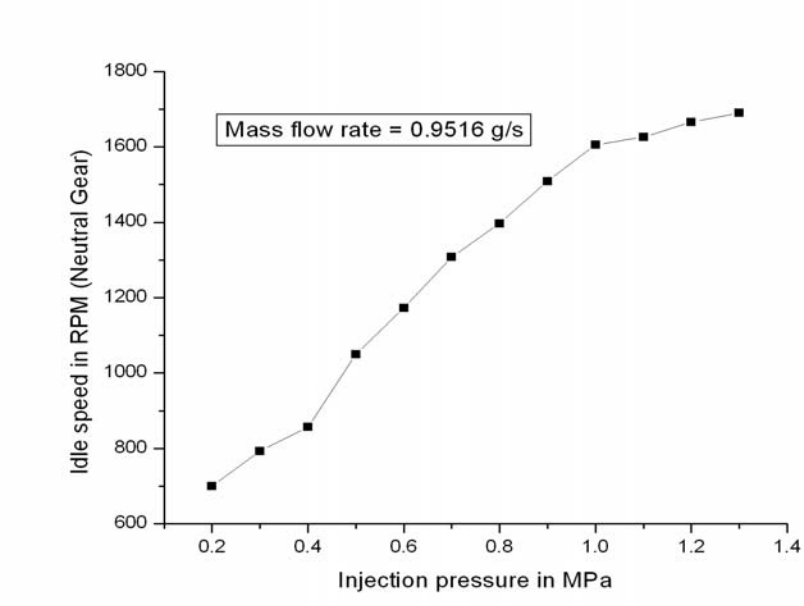

Fig 7.5 shows the neutral gear speed verses different injection pressure for the mass flow rate of 0.9516 g/s.

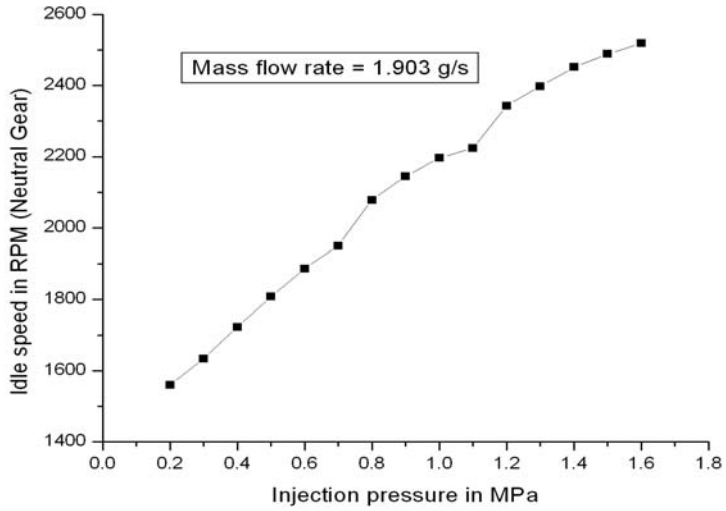

Fig 7.6 shows the neutral gear speed verses different injection pressure for the mass flow rate of 1.903 g/s.

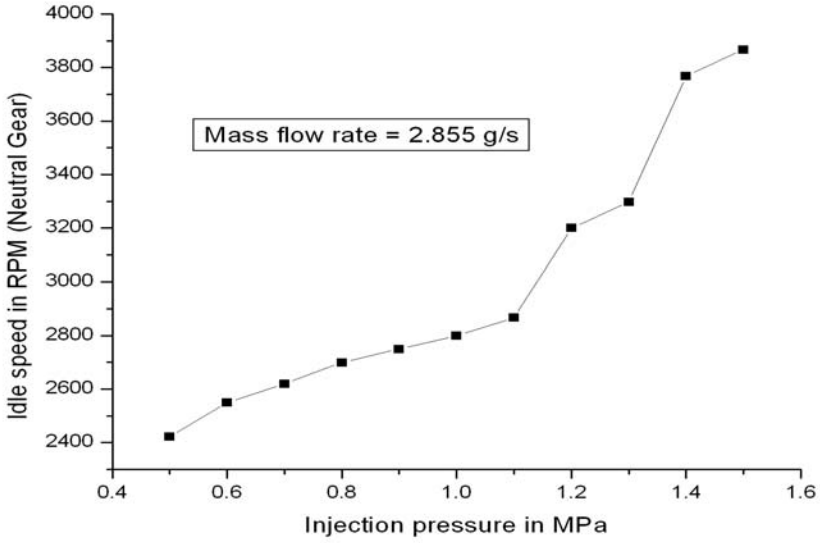

Fig 7.7 shows the neutral gear speed verses different injection pressure for the mass flow rate of 2.855 g/s.

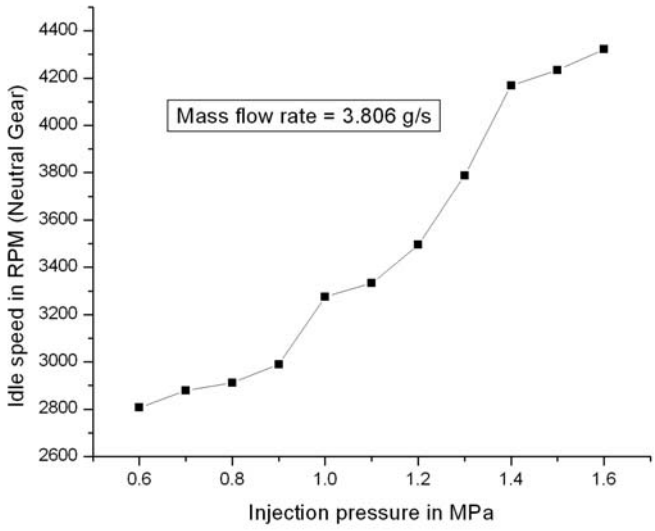

Fig 7.8 shows the neutral gear speed verses different injection pressure for the mass flow rate of 3.806g/s.

The load characteristics, mechanical and thermal efficiencies of the engine can be measured by using rope brake dynamometer setup.

7.5 Optimization of Expansion Engine

After measuring the power output and performance characteristic for different mass flow rate, the expansion engine can be optimized for maximum power output upon after incorporating the followings:

1. Optimization of valve lift and timing by modifying camshaft profile.
2. Increasing the gas injection pressure to the acceptable design pressure force value of the piston, cylinder, crank assembly.
3. Increasing the heat transfer coefficient for the engine body by doing some modification on existing fins arrangement so that it absorbs maximum possible heat from ambient.
4. The expansion engine should be such that, it performs isothermal expansion for the maximum possible stroke length.

7.6 Frost Formation on Heat Exchanger

When the mass flow rate of nitrogen gas to the engine is less than 1.2 g/s, there is no need of blowing air over the heat exchanger. The heat transfer to the LN2 by natural convection is sufficient enough to keep the heat exchanger free from frost formation. When, the mass flow rate exceeds ~ 1.3 g/s there is frost formation on the heat exchanger and this is propagating to the engine faster. Hence, we need to keep the fan running. The fan is blowing air over the heat exchanger at the maximum velocity of 3.4 m/s.

Chapter - 8

Hybrid LN2 Engine, Lightweight Applications, and India

8.1 Advancement on LN2 Powered Engine

The power output range of the LN2 powered engine can be further extended by burning a small amount of petroleum fuels like petrol, diesel, CNG and LNG. As it was discussed in chapter - 3, the Rankine cycle with multistage expansion engines have more efficiency than a single expander. After vaporizing the LN2 with ambient air heat exchanger, its temperature can be further increased by burning a small amount of petroleum fuel in a super heater. The work output from this elevated nitrogen gas is much higher than just ambient heated LN2 cryogenic heat engine, this can be theoretically explained with the help of following modified Otto cycle and Rankine cycles.

8.2 External Combustion Modified Otto Cycle

The schematic of a LN2 prime mover (theoretical concepts), which uses external combustion for increase in nitrogen gas temperature ambient temperature, is shown in Fig 8.1 Maximum system pressure is generated in a fire box which pressurizes individual tubing coils while the isolation valves are closed. Multiple pressure-building coils for each engine cylinder could be used as a means to overcome the longer heating duration required to warm gases in a tube versus that of an internal combustion process. The possibility of preheating the ambient temperature working fluid with combustor and engine exhausts is indicated in Fig 8.1.

The vaporization of the LN2 is accomplished in the same manner as described in earlier power cycle. Pressure drop in the ambient heat exchanger is also accounted for as previously described. After being vaporized and superheated to near ambient temperature (state 2'), the N_2 gas is admitted to individual pressure-building coils having relatively small volume, V_{pbc} as indicated in P-V diagram

Fig.8.2. Constant volume heat addition rapidly increases the internal energy of the gas between states 2 and 3 until the cylinder intake valve is opened. The gas fills the clearance volume and expands against

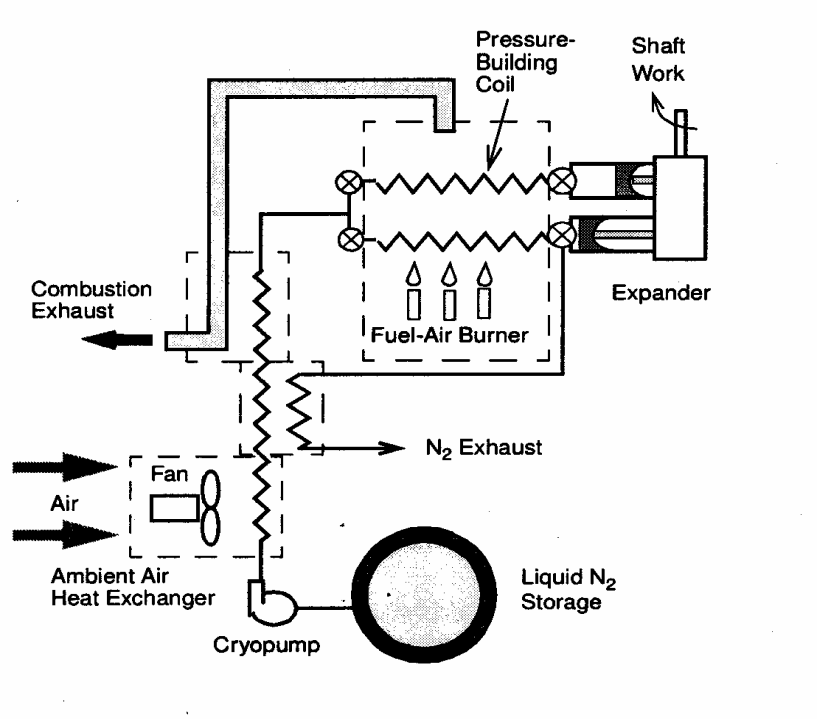

Fig 8.1 Preheating the ambient temperature working fluid with combustor and engine exhausts

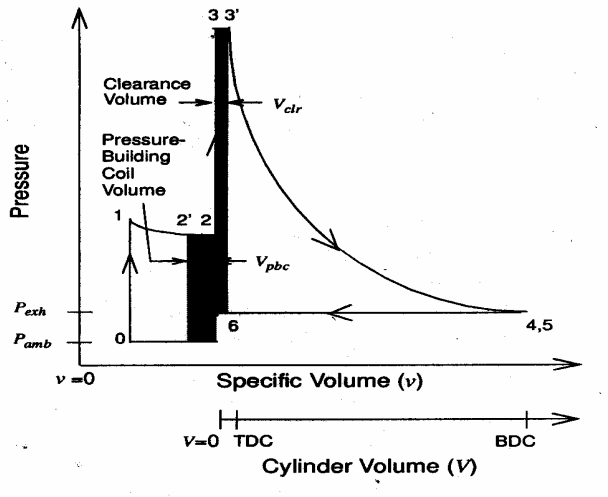

Fig 8.2 P-V diagram for preheated gas cycle

the receding piston until the exhaust pressure reached at state 4 . after the piston reached BDC the exhaust valve is opened and the gas is pushed out of the cylinder and thorough the exhaust system at pressure $P_4 = P_{exh.}$

The work output and input of the expansion and exhaust strokes, respectively, are determined with the help of following equations

$$W_{\exp} = \eta_e W_{34s} = \eta_e c_v T_3 (1 - (P_4 / P_3)^{(\gamma-1)/\gamma}) \quad (8.1)$$

$$W_{exh} = (1/\eta_c)(P_{exh} - P_{amb})(V_1 - V_2) \quad (8.2)$$

$$W_{\exp'} = W_{\exp} - P_{amb}(V_4 - V_3) \quad (8.3)$$

assuming the same mechanical efficiencies as before. The work input from the cryogen pump is determined from equation $W_{pump} = V_0(P_1 - P_0)/\eta_p$ where V_0 is the specific volume of the LN2 in the storage dewar. Even though the heat input to the pressure- building coils tends to reduce the rate of pressure drop during expansion stroke, the expansion process is assumed to be adiabatic. The volume expansion ratio, V4/(Vclr +V_{pbc}), is chosen to fully expand the peak cycle pressure. No injection work is available in this cycle, thus the network is determined from equation

$$W_{net} = W_{\exp'} + W_{inj} - W_{pump} - W_{exh} \quad (8.4)$$

with W_{inj}= 0, since no heat exchange with the exhaust flow is considered, the heat input and fuel mass flow rate are determined from equations

$$q_{23} = C_v(T_3 - T_2) \quad (8.5)$$

where $T_2 = T_1(1 + 1/\eta_c((P_2/P_1)^{(\gamma-1)/\gamma} - 1))$

$$m_f = q_{23}/(\eta_b H_{ihv}) \quad (8.6)$$

η_c = compression mechanical efficiency

η_b = combustion efficiency

H_{lhv} = low heating value of the fuel.

Respectively. Although such a constant volume heater is unusual, this approach does serve as a convenient means to compare potential energetic advantages of internal versus external heat addition process for cryogenic working fluids.

8.3 Cryogenic Rankine Power Cycle

The maximum cycle pressure of a Rankine power cycle using LN2 for the working fluid is usually generated with a cryogen pump (pressure-building circuits are an alternative). The heat addition process is ideally isobaric and expansion process can be adiabatic or isothermal (ideally), depending on peak cycle temperature. The propulsion system schematic in Fig.8.1 applies to an open Rankine cycle, if the isolation valve between ambient heat exchanger and firebox is eliminated. Another version of a cryogenic Rankine power system is shown in Fig 8.3, which illustrates a double expansion with single reheat, along with several heat exchange processes involving the exhausted working fluid. Again the exhaust heat exchange and reheat processes are illustrated for generalization purposes, but the analysis is shown only for the basic cycle without reheat or recuperation.

The pressure –volume history of the cryogenic Rankine power cycle without reheat is shown in Fig 8.4. Significant superheat is provided at nearly constant pressure in the firebox along the path 2-3'. The gas is then injected into the expander and immediately fills the clearance volume as the piston approached TDC. Injection at constant pressure continues until the piston has receded to the point of optimum cutoff, $(V_3 - V_{3'})/V_{4'.}$ producing injection work determined from equation

$$W_{inj} = \eta_c (P_2 - P_{amb}) (V_2 - V_{clr}) \qquad (8.7)$$

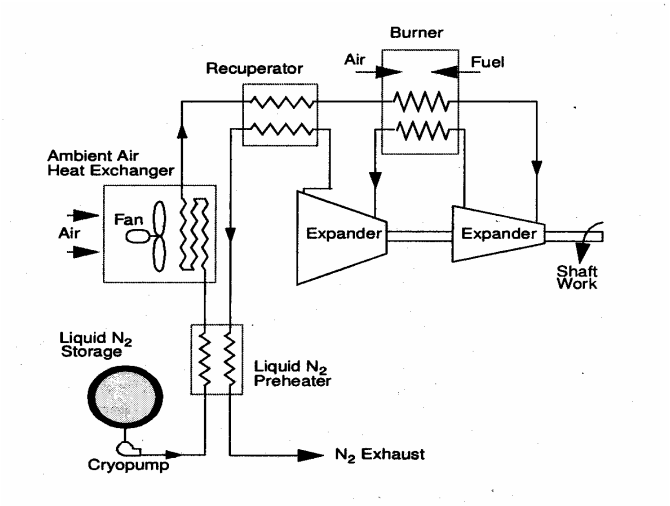

Fig 8.3 Cryogenic Rankine system

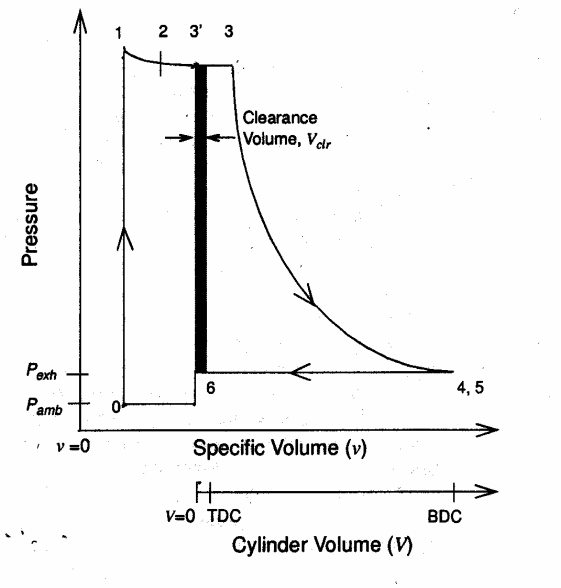

Fig 8.4 pressure –volume diagram of the cryogenic Rankine power cycle

The work of the adiabatic expansion process and exhaust stroke are determined as previously described. Thus the network of the cryogenic Rankine power cycle is determined from equation

$$W_{net} = W_{\exp'} + W_{inj} - W_{pump} - W_{exh} \tag{8.8}$$

Fuel consumption for this power sysle is based on the lowerinh heat value of the fuel H_{ihv} and combustion efficiency η_b as before. However, the total heat input is now for a constant pressure process, i.e.,

$$q_{23'} = C_p(T_3' - T_2) \qquad (8.9)$$

Where Cp is the constant pressure heat capacity. The heat transfer efficiency of the burner is assumed to be the same as the combustion efficiency in the otto cycle. Thus the fuel mass flow rate is determined from equation 7.6 while using the heat input from equation 7.9.

It should also be noted that in the absence of external combustion heat addition this power cycle corresponds to the ZEV mode of operation. Under these circumstances, the cutoff ratio is adjusted for optimum expansion and mechanical efficiencies are assumed to remain constant. The ability to easily switch to ZEV operation by shutting down the fuel flow and adjusting the cutoff is an attractive feature of the cryogenic Rankine cycle just described as well as with the internal and external combustion modified Otto cycles.

8.4 Availability and Cost of Liquid Nitrogen

In near future LN2 is expected to easily available and will become cheap in cities and many other local places in India because;

1. The number of steel industries using Liquid Oxygen for separation of carbon from molten iron is increasing. LN2 is a by-product of LOX tonnage capacity plants.
2. Now a day the requirements for LN2 are increased a lot due to growing fast food preparation and preservation industries.
3. The number of refrigerated trucks on Indian road is expected to increase with LN2 providing refrigeration load.
4. The cost of liquid nitrogen in 1996 is approximately Rs. 30 to 35 in cities like Mumbai and Delhi, If it is bought in bulk quantities. Presently it is

costing only Rs. 6.50 to Rs. 8 and market trend is LN2 price is keep reducing.

5. Many research institutions also use LN2 for different purposes in tons of capacities.
6. LN2 also extensively used in many chemical industries.
7. Once the production capability is increased to accommodate a LN2 powered engines and automobiles, the cost is expected to reduce a lot.

8.5 Application of Liquid Nitrogen Prime Movers

The concept of LN2 powered prime mover using converted four-stroke petrol or diesel engine discussed in this project can be immediately utilized for some of the lightweight applications discussed below. However, as it was discussed in chapter-6 the equipments need to be tested for the better results.

Gengets: Nitrogen engine can used for running gengets, wherever LN2 is used in day today activities. It can be kept well inside the office complex or working environment without causing smog problem to working people.

Forklift and trolley: Presently, many industries are using pneumatic and battery operated forklifts and trolley inside their factory shop floor as a zero pollution prime movers. These prime movers can be easily replaced by LN2 prime movers. Fig 8.5 a and 8.5 b shows photograph of some industrial prime movers, which can be operated using nitrogen engine.

Fig 8.5 (a). Pneumatic Operated Forklift

Lightweight automobiles: All air cooled, four stroke petrol or diesel engine can be very converetded into two stroke cycle liquid nitrogen powered engines.

Fig 8.5 (b) Trolley operated using electric battery

8.6 Environmental Effect of LN2 Powered Prime Movers

The exhaust of the nitrogen engine is only nitrogen. This is good for the environment because nitrogen makes up 78% of the atmosphere. The only pollution created by these nitrogen engines is from the plants that will be used to liquefy the nitrogen. However, in comparison with all of the pollutants that is being created from using gasoline-powered cars and from the plants that make gasoline, this amounts to be very small.

The exhaust temperature of the engine is lower than the ambient temperature. If the number of LN2 powered engines is more, the environment becoming comfortable to human being during hot climatic conditions unlike I.C. engines making the environment warmer and uncomfortable to Human being.

The liquid nitrogen available in the market is usually better than 98% pure. The atmosphere may be impure in comparison to the nitrogen gas exhaust from the LN2 engine. This makes the environment cleaner, if more engines are made to run on LN2, it makes the environment better with Negative contamination.

8.7 Advantages of LN2 Engine over Battery Car

The main reasons why the nitrogen cars are better are that the fuel weighs less than the batteries. In addition, it only takes minutes to refuel a liquid nitrogen car compared to the hours it takes to recharge an electric car. Liquid nitrogen cars run at faster speeds, and the cost of going one mile in a nitrogen car is less than in an electric car. As with all alternative energy storage media, the energy density (W-hr/kg) of liquid nitrogen is relatively low when compared to gasoline but better than that of readily available battery systems. Studies indicate that liquid nitrogen automobiles will have significant performance and environmental advantages over electric vehicles. Cryogenic Heat engine car could meet or exceed the range and performance of a battery powered car; therefore, nitrogen powered vehicles could compete for a share of the zero emission car concepts available in the market. Furthermore, a liquid nitrogen car

will be much lighter and refilling its tank will take only 10-15 minutes, rather than the several hours required by most electric car concepts. Motorists will fuel up at filling stations very similar to today's gasoline stations.

8.8 Indian Climatic Conditions

The maximum average temperature of Nagpur city is 32.3^{o}C, which is approximately 15^{o}C more than average temperature of Texas, USA. This increases the local heat transfer coefficient by 2.8% (refer Appendix ‘B”) for velocity of air flowing over the heat transfer surface assumed to be 6.5 m/s (air blown by a ordinary fan over heat transfer surface). However, the velocity of air flowing over heat transfer area in the case of automobiles is very high. Climatic conditions India is favorable compared to other European and American countries (ref; appendix “C’)

Conclusion

The concept of liquid nitrogen powered prime mover using modified four-stroke cycle engine as an expansion engine and monochlorodifluoromethane refrigerant heat exchanger is demonstrated. It is also shown that the efficiency of the system can be improved a lot by optimization of expansion engine, optimization of LN2 evaporative system and dual cycle concept.

Presently, liquid nitrogen is easily available in Indian market and becoming cheaper compared to earlier years. The exhaust gas temperature is lower than ambient temperature and it is being a cryogenic heat engine, its efficiency increases with increase in ambient temperature. These reasons favors this LN2 powered prime mover concept for India and demanding further research and development. However, this concept can be immediately implemented in some lightweight prime mover applications in places like airport, hospitals, factories and also light automobiles.

References

1. Knowlen, C., Hertzberg, A etal “Cryogenic Automotive Propulsion’ AIAA 94-4224, 1994.
2. C.A. ordonez, M.C.Plummerr, R.F.Reidy, “Cryogenic Heat Engines for powering zero emission Vehicles” ASME exposition 2001.
3. C.Knowlen, A.T.Mattick, etal “Ultra Low emission Liquid Nitrogen Automobile” SAE paper 1999-01-2932, 1999.
4. Knowlen, C., Mattick, etal “ High Efficiency Energy Conversion systems for Liquid Nitrogen Automobiles” SAE paper 981898, 1998.
5. J.Williams, C.Knowlen etal. “ Frost Free Cryogenic Heat Exchanger for Automotive Propulsion” ASME/SAE/ASEE joint prop. Conf. 1997.
6. University of Washington web site
7. University of North Texas web site

Appendix “A”

Inner vessel end plates Material;S.S.304, thickness;12 mm

```
MPLIST,1,1,1
  Label    Name   Temp/BH_Cr        Value
A   1       EX            0     1.900000e+011
A   1      NUXY           0     2.900000e-001
A   1      GXY            0     7.500000e+010
A   1      ALPX           0     1.800000e-005
A   1      DENS           0     8.000000e+003
A   1       C             0     5.000000e+002
A   1       KX            0     1.600000e+001
A   1   MPERM_R           0     1.000000e+000

RCLIST,1,1,1
                    Real Constant Sets

  Real Constant Set :   1  (ACTIVE)
  Associated Element Group :   1  ( SHELL3 )

    Rc1  : Thickness   . . . . . . . . . . . . . =  1.200000e-002
    Rc2  : Temperature gradient . . . . . . . . . =  0.000000e+000
    Rc3  : Foundation stiffness . . . . . . . . . =  0.000000e+000
    Rc4  : Unused real constant . . . . . . . . . =  0.000000e+000
    Rc5  : Prestress value (NSTAR only)  . . . . . . =  0.000000e+000
    Rc6  : Prestrain value (NSTAR only)  . . . . . . =  0.000000e+000
```

Outer vessel end plates Material;S.S.304, thickness;8 mm

```
MPLIST,1,1,1
  Label    Name   Temp/BH_Cr        Value
A   1       EX            0     1.900000e+011
A   1      NUXY           0     2.900000e-001
A   1      GXY            0     7.500000e+010
A   1      ALPX           0     1.800000e-005
A   1      DENS           0     8.000000e+003
A   1       C             0     5.000000e+002
A   1       KX            0     1.600000e+001
A   1   MPERM_R           0     1.000000e+000

RCLIST,1,1,1
                    Real Constant Sets

  Real Constant Set :   1  (ACTIVE)
  Associated Element Group :   1  ( SHELL3 )
```

Rc1 : Thickness . . . . . = 8.000000e-003
Rc2 : Temperature gradient . . . . . = 0.000000e+000
Rc3 : Foundation stiffness . . . . . = 0.000000e+000
Rc4 : Unused real constant . . . . . = 0.000000e+000
Rc5 : Prestress value (NSTAR only) . . . . . = 0.000000e+000
Rc6 : Prestrain value (NSTAR only) . . . . . = 0.000000e+000

Appendix - 'B"

Problem Formulation

1) Air at 293 K is flowing over a flat plate at 125K (boiling point temperature of LN2 at 33.8 bar) at a velocity of 6.5 m/s.

Local heat transfer coefficient calculation

$R_{ex} = U.x/\nu$

$$\mathbf{N_u = h_x.x/k = 0.332\ (R_{ex})^{0.5}\ (P_r)^{0.333}}$$

X=0.4 m, U = 6.5 m/s

Film temperature (T_f) = 209 K

Properties of air considered at film temperature

ν = 0.0000084 m^2/s, thermal conductivity (k) = 0.0189 w/mK

h_x = 7.74 w/mK

2) Air at 308 K is flowing over a flat plate at 125 K (boiling point temperature of LN2 at 33.8 bar) at a velocity of 6.5 m/s.

Local heat transfer coefficient calculation

$R_{ex} = U.x/\nu$

$$\mathbf{N_u = h_x.x/k = 0.332\ (R_{ex})^{0.5}\ (P_r)^{0.333}}$$

X=0.4 m, U = 6.5 m/s

Film temperature (T_f) = 216.5 K

Properties of air considered at film temperature

ν = 0.000009 m^2/s, thermal conductivity (k) = 0.019 w/mK

h_x = 7.52 w/mK

The difference = (7.74-7.52)/7.74 = 2.84%

APPENDIX 'C'

NORMAL MONTHLY TEMPERATURE (Deg. C)

(January, July, October | Back to Normal Temperature maps)

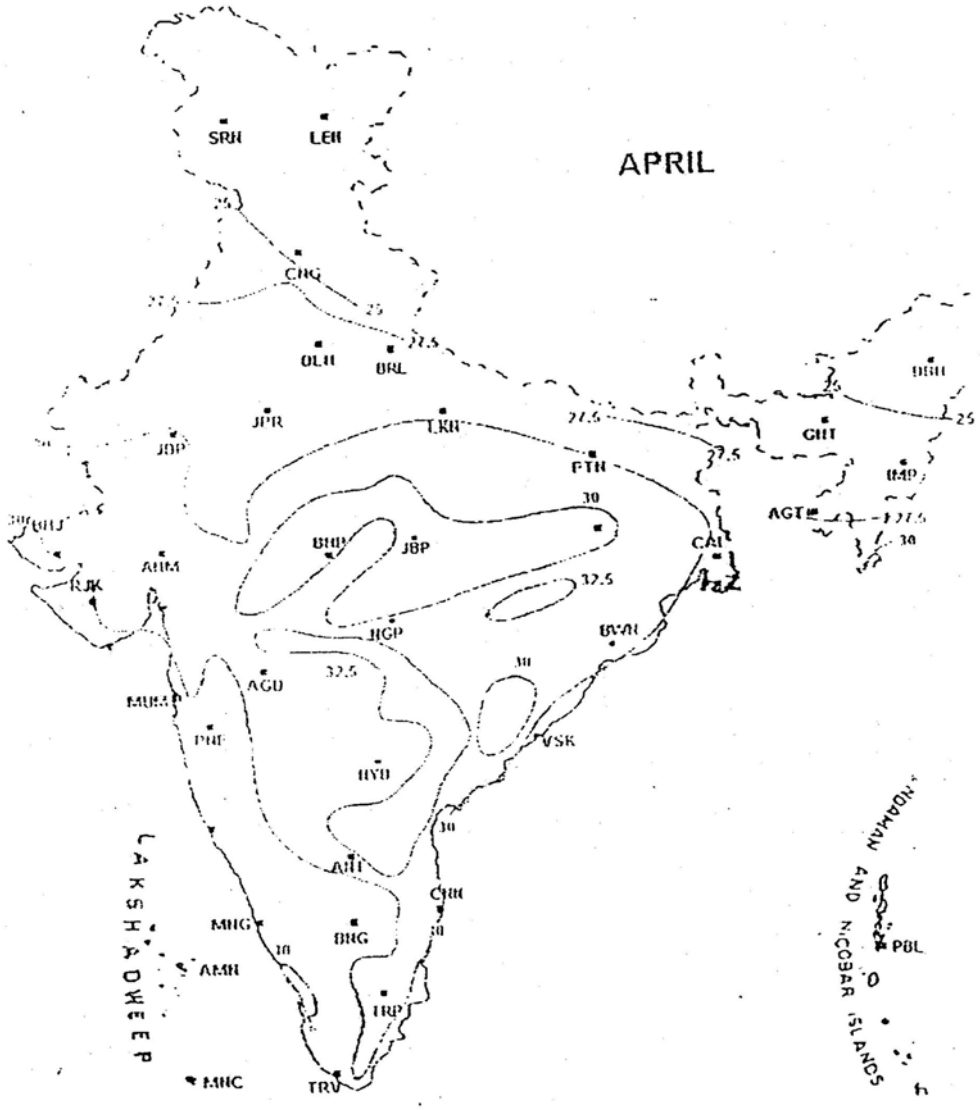

CHENNAI

Month	Mean Temperature °C		Mean Total Rainfall (mm)	Mean Number of Rainy Days
	Daily Minimum	Daily Maximum		
Jan	20.6	28.4	16.2	1.0
Feb	21.2	29.9	3.7	0.3
Mar	23.1	31.9	3.0	0.2
Apr	25.9	33.6	13.6	0.7
May	27.6	36.4	48.9	1.6
Jun	27.2	36.6	53.7	4.1
Jul	25.9	34.7	97.8	7.3
Aug	25.3	33.9	149.7	8.5
Sep	25.3	33.5	109.1	6.6
Oct	24.3	31.4	282.7	10.2
Nov	22.8	29.2	350.3	10.1
Dec	21.6	28.1	138.2	5.5

MUMBAI

Month	Mean Temperature °C		Mean Total Rainfall (mm)	Mean Number of Rainy Days
	Daily Minimum	Daily Maximum		
Jan	16.4	30.6	0.6	0.1
Feb	17.3	31.3	1.5	0.1
Mar	20.6	32.7	0.1	0.0
Apr	23.7	33.1	0.6	0.1
May	26.1	33.3	13.2	1.0
Jun	25.8	31.9	574.1	14.9
Jul	24.8	29.8	868.3	24.0
Aug	24.5	29.3	553.0	22.0
Sep	24.0	30.1	306.4	13.7
Oct	23.1	32.9	62.9	3.2
Nov	20.5	33.4	14.9	1.1
Dec	18.2	32.0	5.6	0.4

NAGPUR

Month	Mean Temperature °C		Mean Total Rainfall (mm)	Mean Number of Rainy Days
	Daily Minimum	Daily Maximum		
Jan	12.4	28.6	10.2	1.0
Feb	15.0	32.1	12.3	1.1
Mar	19.0	36.3	17.8	1.5

Apr	23.9	40.2	13.2	1.4
May	27.9	42.6	16.3	1.2
Jun	26.3	37.8	172.2	9.0
Jul	24.1	31.5	304.3	15.0
Aug	23.6	30.4	291.6	14.4
Sep	22.9	31.8	194.4	9.4
Oct	19.8	32.6	51.4	2.8
Nov	14.9	30.4	11.8	0.7
Dec	12.1	28.2	17.2	0.8

33·5

NEW DELHI

Month	Mean Temperature °C		Mean Total Rainfall (mm)	Mean Number of Rainy Days
	Daily Minimum	Daily Maximum		
Jan	7.3	21.1	20.3	1.7
Feb	10.1	24.2	15.0	1.3
Mar	15.4	30.0	15.8	1.2
Apr	21.5	36.2	6.7	0.9
May	25.9	39.6	17.5	1.4
Jun	28.3	39.3	54.9	3.6
Jul	26.6	35.1	231.5	10.0
Aug	25.9	33.3	258.7	11.3
Sep	24.4	33.9	127.8	5.4
Oct	19.5	32.9	36.3	1.6
Nov	12.8	28.3	5.0	0.1
Dec	8.2	23.0	7.8	0.6

KOLKATA

	Mean Temperature °C			
	Daily	Daily		
Jan	13.9	26.6	16.8	0.9
Feb	16.9	29.7	22.9	1.5
Mar	21.7	34.0	32.8	2.3
Apr	25.1	36.3	47.7	3.0
May	26.4	36.0	101.7	5.9
Jun	26.5	34.1	259.9	12.3
Jul	26.1	32.2	331.8	16.8
Aug	26.1	32.0	328.8	17.2

Aug	26.1	32.0	328.8	17.2
Sep	25.8	32.2	295.9	13.4
Oct	24.0	31.9	151.3	7.4
Nov	18.9	29.8	17.2	1.1
Dec	14.3	27.0	7.4	0.4

Climate At A Glance

April Temperature
Texas

April 2004: 64.5 degF Rank: 11

April 1980 - 2004 Average = 65.09 degF
April 1980 - 2004 Trend = 0.50 degF / Decade

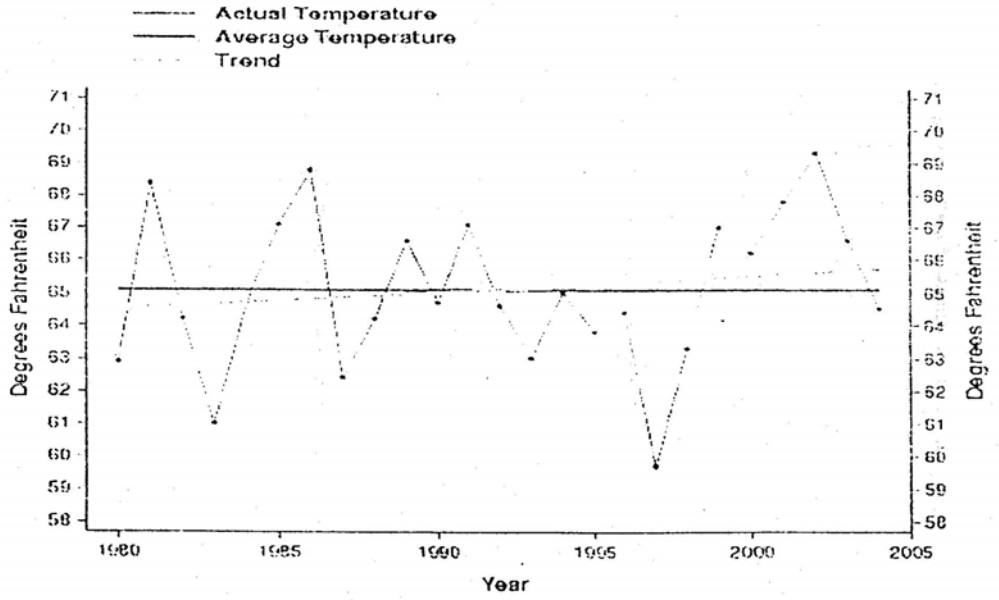

NCDC / Climate At A Glance / Climate Monitoring / Search / Help

This graph was dynamically generated 01 /24 /2005 at 14:10:54
via http://www.ncdc.noaa.gov/oa/climate/research/cag3/NA.html
Please send questions to Karin.L.Gleason@noaa.gov
Please see the NCDC Contact Page if you have questions or comments.

SATURATED LIQUID NITROGEN

SI Units

Temp. (K)	P_{sat} (kPA)	ρ_f (kg/m³)	C_p (kJ/kg K)	μ (μPa s)	k (mW/m K)	h_{fg} (kJ/kg)	Pr	σ_f (mN/m)	ε
65	17.4	860.9	2.008	278	158.7	214.0	3.52	11.66	1.46273
70	38.5	840.0	2.024	229	149.9	208.3	2.97	10.48	1.45077
75	76.0	818.1	2.042	173	143.0	202.3	2.47	9.30	1.43652
77.36	101.3	807.3	2.051	158	139.6	199.3	2.32	8.75	1.43164
80	136.7	795.1	2.063	141	136.2	195.8	2.14	8.22	1.42432
85	228.4	771.0	2.088	119	129.3	188.7	1.922	7.18	1.40994
90	359.8	745.6	2.122	101	122.4	180.9	1.803	6.12	1.39477
95	549.8	718.6	2.170	93	115.5	172.0	1.747	5.08	1.37867
100	777.8	689.6	2.240	85	108.5	161.6	1.755	4.04	1.36146
105	1083.6	657.7	2.350	78	101.1	149.4	1.813	---	1.34280
110	1467.2	621.7	2.533	71	93.6	135.0	1.976	---	1.32221
115	1941.4	579.3	2.773	68	84.7	117.3	2.19	---	1.29854
120	2512.9	524.9	2.930	65	74.6	94.3	2.54	---	1.26903
125	3201.4	436.8	3.124	62	61.5	54.9	3.14	---	1.21553

U.S. Customary Units

Temp. (°R)	P_{sat} (psia)	ρ_f (lb_m/ft^3)	C_p (Btu/lb_m °R)	μ (lb_m/ft hr)	k (Btu/hr ft °R)	h_{fg} (Btu/lb_m)	Pr	σ_f (lb_f/ft)	ε
115	2.08	53.9	0.475	0.705	0.0925	92.1	3.30	8.19×10^{-4}	1.46526
120	3.34	53.3	0.481	0.624	0.0900	91.2	3.32	7.71×10^{-4}	1.45885
130	7.65	51.9	0.488	0.477	0.0850	88.7	2.71	6.81×10^{-4}	1.44517
139.3	14.70	50.4	0.490	0.382	0.0807	85.7	2.32	6.00×10^{-4}	1.43164
150	28.13	48.6	0.495	0.305	0.0759	82.0	2.00	5.14×10^{-4}	1.41482
160	42.38	46.8	0.502	0.259	0.0715	78.2	1.83	4.35×10^{-4}	1.39822
170	59.9	45.0	0.515	0.227	0.0672	74.1	1.75	3.57×10^{-4}	1.38052
180	82.7	43.1	0.536	0.203	0.0628	69.5	1.75	2.77×10^{-4}	1.36146
190	102.7	41.0	0.570	0.182	0.0581	64.0	1.83	2.04×10^{-4}	1.34064
200	127.0	38.4	0.613	0.174	0.0530	57.0	2.00	1.10×10^{-4}	1.31728
210	160.6	35.1	0.663	0.163	0.0470	47.2	2.38	0.76×10^{-4}	1.28964
220	206.9	30.4	0.719	0.154	0.0399	33.3	2.79	0.25×10^{-4}	1.25163

GASEOUS NITROGEN AT 101.3 kPA (1 atm)

SI Units

Temp. (K)	ρ (kg/m³)	C_p (kJ/kg K)	μ (μPa s)	k (mW/m K)	Pr	ε
77.36	4.604	1.082	5.41	7.23	0.811	1.00217
100	3.481	1.065	6.98	9.33	0.797	1.00164
125	2.769	1.055	8.53	11.64	0.776	1.00130
150	2.289	1.047	10.05	13.77	0.767	1.00105
175	1.955	1.044	11.54	15.85	0.759	1.00093
200	1.711	1.043	12.95	18.02	0.750	1.00080
225	1.519	1.043	14.29	20.05	0.743	1.00071
250	1.367	1.042	15.55	22.10	0.733	1.00064
275	1.242	1.042	16.73	24.04	0.725	1.00058
300	1.142	1.042	17.86	25.79	0.722	1.00054

U.S. Customary Units

Temp. (°R)	ρ (lb_m/ft³)	C_p (Btu/lb_m °R)	μ (lb_m/ft hr)	k (Btu/hr ft °R)	Pr	ε
139.3	0.287	0.259	0.01309	0.00418	0.811	1.00217
180	0.265	0.258	0.01409	0.00445	0.807	1.00200
225	0.1939	0.254	0.01860	0.00596	0.788	1.00147
270	0.1532	0.251	0.0225	0.00741	0.771	1.00116
315	0.1264	0.250	0.0267	0.00876	0.761	1.00097
360	0.1071	0.249	0.0306	0.01013	0.752	1.00083
405	0.0930	0.249	0.0342	0.01145	0.744	1.00072
450	0.0821	0.249	0.0376	0.01273	0.737	1.00064
495	0.0734	0.249	0.0408	0.01405	0.735	1.00058
540	0.0662	0.249	0.0439	0.01494	0.732	1.00054